Received Signal Strength Calibration for Wireless Local Area Network Localization

by

Diego Felix
B.Sc. Universidad Catolica 2006, Quito, Ecuador

A Thesis Submitted in Partial Fullfillment of the
Requirements for the Degree of

MASTER OF APPLIED SCIENCE

in the Department of Electrical and Computer Engineering

Received Signal Strength Calibration for Wireless Local Area Network Localization

by

Diego Felix
B.Sc. Universidad Catolica 2006, Quito, Ecuador

Supervisory Committee

Dr. Michael McGuire (Department of Electrical and Computer Engineering)
Supervisor

Dr. Mihai Sima (Department of Electrical and Computer Engineering)
Departmental Member

Dr. Kui Wu (Department of Computer Science)
Outside Member

Supervisory Committee

Dr. Michael McGuire (Department of Electrical and Computer Engineering)
Supervisor

Dr. Mihai Sima (Department of Electrical and Computer Engineering)
Departmental Member

Dr. Kui Wu (Department of Computer Science)
Outside Member

Abstract

Terminal localization for indoor Wireless Local Area Networks (WLAN) is critical for the deployment of location-aware computing inside of buildings. The purpose of this research work is not to develop a novel WLAN terminal location estimation technique or algorithm, but rather to tackle challenges in survey data collection and in calibration of multiple mobile terminal Received Signal Strength (RSS) data. Three major challenges are addressed in this thesis: first, to decrease the influence of outliers introduced in the distance measurements by Non-Line-of-Sight (NLoS) propagation when a ultrasonic sensor network is used for data collection; second, to obtain high localization accuracy in the presence of fluctuations of the RSS measurements caused by multipath fading; and third, to determine an automated calibration method to reduce large variations in RSS levels when different mobile devices need to be located. In this thesis, a robust window function is developed to mitigate the influence of outliers in survey terminal localization. Furthermore, spatial filtering of the RSS signals to reduce the effect of the distance-varying portion of noise is proposed. Two different survey point geometries are tested with the noise reduction technique: survey points arranged in sets of tight clusters and survey points uniformly distributed over the network area. Finally, an affine transformation is introduced as RSS calibration method between mobile devices to decrease the effect of RSS level variation and

an automated calibration procedure based on the Expectation-Maximization (EM) algorithm is developed. The results show that the mean distance error in the survey terminal localization is well within an acceptable range for data collection. In addition, when the spatial averaging noise reduction filter is used the location accuracy improves by 16% and by 18% when the filter is applied to a clustered survey set as opposed to a straight-line survey set. Lastly, the location accuracy is within 2m when an affine function is used for RSS calibration and the automated calibration algorithm converged to the optimal transformation parameters after it was iterated for 11 locations.

Table of Contents

List of Figures

List of Tables

List of Acronyms

CDF Cumulative Distribution Function

ECS Engineering and Computer Science building

EM Expectation Maximization

FIR Finite Impulse Response

GPS Global Positioning System

IF Influence Function

IIR Infinite Impulse Response

LoS Line-of-Sight

MLE Maximum Likelihood Estimator

MSE Mean Square Error

MMSE Minimum Mean Square Error

NLoS Non-Line-of-Sight

PDF Probability Density Function

RF Radio Frequency

RMSE Root Mean Squared Error

RSS Received Signal Strength

SNR signal-to-noise ratio

TDoA Time Difference of Arrival

SVD Singular Value Decomposition

WAP Wireless Access Points

WLAN Wireless Local Area Networks

Acknowledgements

Foremost I would like to thank my research supervisor Dr. Michael McGuire for his guidance and support. I truly admire him for his native intelligence and disposition to teach. I would also like to thank my parents and sister for supporting me in every endeavor in my life. Thanks to the friends I made during my tenure at the University of Victoria, in particular, Ami, Eugene, Ranjit, Masoud, Deepali, Ping, Goran and Stephanie. I also want to express my gratitude to the members of my supervisory committee and the technical and office staff in the Electrical and Computer Engineering Department.

Chapter 1

Introduction

Over the past few years the cost of wireless communications hardware has decreased significantly. As a result, telecommunications companies have widely deployed Wireless Local Area Networks in indoor environments such as university campuses, airports, hotels, hospitals. Wireless modems have been integrated into very small and highly portable devices, such as laptops and cellular phones. The growing sensing and computing capabilities of these devices has ignited a new form of computing called *location-aware computing* [1]. Location aware computing provides applications with knowledge of the physical location where the computation is taking place [2]. Examples of indoor location-aware services include location-based network management, access and security [3–5], automatic resource allocation [3,6], location-sensitive information delivery [7], and context-awareness [8].

A fundamental task to facilitate the delivery of location-aware services is accurately determining the position of the computing device. The standard location sensing system in North America is the well-known satellite navigation based Global Positioning System (GPS). This system allows mobile receiver units to compute their position by measuring times-of-arrival of the radio signal from navigation satellites [9]. Typical accuracies for outdoor localizations are within a few meters of a terminal's true location. Nevertheless, Global Positioning System (GPS) location performance is severely hindered in dense urban areas and indoor environments, since GPS satellite signals are received only intermittently in these locations [10–12].

Consequently, several indoor positioning systems have been developed in order to tackle this deficiency [13, 14]. All of these systems involve gathering data by sensing

a physical quantity related to the signal propagation and using it to calculate a location estimate. Some of the earliest systems rely on periodic infrared light pulses sent between a transmitter and a receiver [15–17]. More recent work has led to the development of positioning systems based on radio signals. Signal characteristics used for location estimation purposes include Time of Arrival (ToA) [18, 19], Time Difference of Arrival (TDoA), Angle of Arrival (AoA) [20] and Received Signal Strength (RSS) [21–29]. The most popular signal characteristic measured for a WLAN positioning system is RSS since it can be obtained from the Network Interface Card (NIC) available in most mobile computing devices without modification. Thus, this kind of systems constitute a cost-effective solution for localization in indoor environments [30]. However, the intention of this thesis is not to formulate a new location fingerprinting algorithm, but to address problems present in survey data collection and in RSS calibration for different mobile devices.

1.1 WLAN Localization

The purpose of WLAN localization is to implement a rule $f(\cdot) : \mathbb{R}^L \rightarrow \mathbb{R}^2$ that relates the measured RSS vector, $\boldsymbol{v}$, from L Wireless Access Points (WAP)s to a spatial location in 2D Cartesian coordinates $\boldsymbol{\theta} = (x, y)$ [27]. In ideal indoor environments, i.e. where free space propagation exists, the received signal power is inversely proportional to the square of the distance between transmitter and receiver. In non-ideal indoor environments, the relation between distance and RSS measurements is highly nonlinear due to conditions such as multipath and shadow fading, NLoS propagation and interference from other devices [31]. Due to these unpredictable propagation characteristics the RSS-position relation cannot be formulated explicitly. Therefore, WLAN Positioning plataforms use a method known as *location fingerprinting* to characterize the RSS-position relation in an implicit manner. Location fingerprinting is created

under the assumption that each position in a certain environment has a unique Radio Frequency (RF) signature [32]. This technique consists of two phases. In the first phase, a set of location fingerprints, called a *training* or *survey set*, is collected with the intention of obtaining a representation of spatial RSS properties of the operating area. The location fingerprints and their respective location information (i.e. position coordinates) are stored in a database. The second phase entails comparing a new set of location fingerprints, called a *test* or *data set*, to the training record at each survey point. The fingerprint or *pattern* with the closest match in the database becomes then the position estimate.

On the other hand, in location fingerprinting the geometric configuration of WAPs can affect the localization accuracy. As a result, the selection of WAPs to be used in location estimation is a key issue. Since only RSS measurements from 3 WAPs are needed for location estimation, the use of measurements from all available WAPs will increase the computational complexity of the estimation algorithm. Due to the RSS dependence on the distance between the mobile terminal and the WAPs, correlated measurements might be reported, which may lead to biased estimates. Consequently, a need for a WAP selection method arises, which will choose a subset of all *seen* WAPs to be used in localization [30]. The most common WAPs selection method is to choose the WAPs that provide with the highest RSS readings at a given location [33].

Furthermore, a non-parametric kernel or Parzen window method will be utilized as estimation algorithm in this thesis to deal with a lack of a known model relating the RSS measurements to the location to be estimated. The kernel window is used for approximating the mobile terminal's joint Probability Density Function (PDF) of RSS and location information from mobile terminal data. Every component function is centered at a survey measurement, thus points closer to several survey points will have higher probability than positions further away from survey points [34].

1.2 Technical Challenges

In a location fingerprinting system there are some technical difficulties involving the survey set data collection and in multiple mobile terminal RSS calibration that need to be considered. To begin with, there is a high cost associated with the survey data collection phase. Conventional measuring methods with rulers and tapes to define survey points in a large area involves a great deal of work [35]. In this thesis, a sensor network is proposed to collect survey locations in a rapid and inexpensive manner. The beacon sensors will be placed on walls, as opposed to on the ceiling as in previous work [35], to locate a listener sensor in hallways of a university building. The first technical challenge of this work arises due to the inability of the acoustic sensors to handle reflections [36]. Ultrasound reflections off walls create outliers in the distance measurements [37], i.e. there are a few values in the sample that are far away from the bulk of the data. The presence of outliers in the measurements causes a gross error in the listener sensor localization. In order to reduce the damage caused by outliers in the sensor location estimation process a robust window function is proposed.

Another challenge faced in this work is that the accuracy of a WLAN fingerprinting system is limited by measurement noise which can cause two separate locations to appear identical with respect to RSS measurements. This noise is created by thermal noise and random variations of the RSS created by multipath propagation. Past efforts on noise removal have processed the RSS measurements over time, with several filters being proposed [38–42]. However, if a mobile terminal is immobile during data collection, much of the measurement noise created by multipath propagation is time-invariant over the period of survey data collection [31,43]. Time-averaging techniques do not remove this component of the noise. In this thesis, a filter is proposed which averages signals over space during the collection of the RSS survey data.

A third challenge in a WLAN fingerprinting platform appears when a new mobile device is introduced into the measuring environment for location purposes. It has been reported that there are variations in the RSS measurements if two different WLAN cards are used to collect data [32, 33, 44]. In particular, the signal levels in different devices differ mainly due to the different number of antennas and the diversity schemes employed in each device, the orientation of the device, and the receiver sensitivity and granularity. This variability in the RSS data calls for the development of a calibration method to match the RSS levels between different mobile devices. In this thesis, the RSS variations between two laptops and between a laptop and several handsets is analyzed to obtain an affine transformation as a calibration method.

1.3 Thesis Contributions

The specific contributions of the research presented in this thesis are the following:

1. **Robust Window:** The development of a robust window function to mitigate the influence of outliers in the distance measurement vectors when performing ultrasonic radio-acoustic localization. The proposed window is a modification of the original Huber Window based on distance measurements obtained from the sensor network. It will be shown that the proposed window function outperfoms the conventional Huber window in terms of robustness and that this new window allows sensor localization with accuracy levels far better than necessary for radio location survey collection.

2. **Noise Removal:** The second contribution of this thesis is a technique for noise reduction in the survey set. A spatial domain noise reduction technique to reduce time-invariant measurement noise caused by multipath propagation is introduced. It will be demonstrated that averaging over space provides a substantial accuracy improvement. In this thesis, we propose the collection of

survey points in uniformly distributed tight clusters of locations, as opposed to at locations uniformly distributed over the network area. It will be shown that survey data collected in tight clusters of locations provide superior accuracy compared to survey points uniformly distributed in the network area because the noise removal technique is more efficient with this type of survey data collection. A cross-validation technique is presented to find the parameters of the noise removal and location estimation algorithms from the survey data.

3. **Automated Calibration:** The last contribution of this thesis is a calibration method of RSS measurements from different mobile terminals. First, the development of an algorithm to estimate the RSS measurements of a data set using the locations of the mobile terminal is presented. Second, an affine transformation as a calibration technique between RSS measurements of two laptops, and a laptop and several mobile phones is introduced. A localization accuracy of less than 2m is achieved when the affine transformation is used. Third, an automated calibration method is developed based on the Expectation-Maximization algorithm. This method constitutes an online process that needs a few locations to determine the optimal transformation parameters.

1.4 Thesis Organization

The remainder of the thesis is arranged as follows. Chapter 2 describes the survey data collection technique with the use of a ultrasonic sensor network and explains the sensor localization algorithm. An introduction of Robust Statistics is provided as a method for outlier rejection in the sensor distance measurements. The conventional Huber window is presented and a modification of this window is developed for our specific problem. Chapter 3 presents a noise removal algorithm for the survey data set. This noise removal algorithm is based on both time domain averaging and spatial

averaging of the filter.

Chapter 4 presents the survey-based radiolocation algorithm based on a Parzen Window Estimator. A method for determining the values of the location estimation algorithm from survey data is also presented. Chapter 5 describes the solution of calibration of the radiolocation system for different types of radio terminals. Methods for determining the parameters of affine transformations between RSS signal vectors for different terminals are presented. Chapter 6 concludes this thesis and presents avenues for future research.

Chapter 2
Data Collection

As mentioned in Section 1.1, the purpose of survey data collection is to obtain a representation of the spatial properties of the RSS or a so-called *radio map* of the measuring area. During the data collection phase, an ultrasonic sensory network is used for obtaining accurate true locations for a set of survey points, while the WLAN provides RSS measurements. This sensor network allows for a fast and inexpensive data collection. The ultrasonic sensors are only used for localization during survey data collection. After the completion of the data collection phase, the acoustic sensors are removed. In the following sections, a brief description of operation of the ultrasonic sensor network is given along with the proposed robust window function for sensor localization. The main objective of the proposed robust window is to prevent a gross error in listener localization produced by undetected outliers.

2.1 Ultrasonic Sensor Network

The ultrasonic sensor network is composed of a number of transceivers called Crickets [45]. A Cricket sensor unit acts either as a listener or a beacon. A listener Cricket is located at the mobile terminal and the remaining Crickets act as beacon sensor nodes placed at known locations. The listener node measures the time difference in the arrival of the RF and ultrasonic signals received from the beacon node. The beacons periodically transmit simultaneous RF pulses at 433 MHz and narrow ultrasonic pulses at 40 kHz. The ultrasonic signal lags behind the RF signal when both signals propagate, since the speed of an RF signal is much faster than the speed of sound. When a listener receives the RF pulse from some beacon, followed by an

ultrasonic signal, it measures the time interval between the start of the RF pulse and the arrival of the ultrasound signal at the listener [45, 46]. The distance d between the listener and each beacon Cricket is calculated based on this time difference from:

$$\Delta T = \frac{d}{v_{US}} - \frac{d}{v_{RF}}, \tag{2.1}$$

where v_{US} is the speed of sound and v_{RF} is the speed of the RF pulse [45]. The listener sends the computed distances to a laptop computer via a serial cable [35].

2.2 Cricket Localization Algorithm

The location of the listener sensor is estimated with a Maximum Likelihood Estimator (MLE). The errors in the distance measurements between the listener Cricket and beacon Crickets are assumed to be equal variance, zero mean and independent Gaussian random variables for each beacon sensor. The central limit theorem supports the idea that assuming a normal distributiom is a good assumption in this case. The MLE becomes then a least-squares optimization, that is:

$$(x, y, z) = \arg \min_{(x,y,z)} \sum_{k=1}^{N} \left[d_k - \hat{d}_k(x, y, z) \right]^2 \tag{2.2}$$

where $\hat{d}_k(x, y, z) = \sqrt{(x - x_k)^2 + (y - y_k)^2 + (z - z_k)^2}$; x, y, and z are the estimated coordinates of the listener; x_k, y_k, and z_k are the coordinates of the k_{th} beacon; $\hat{d}_k$ is the estimated distance between the listener and the k_{th} beacon; and d_k is the distance between the listener and the k_{th} beacon measured by the ultrasonic sensors.

In typical survey measurements z is known, since z represents the height of the cart where the mobile terminal and listener are located. Thus, there are only two unknowns x and y to be determined and the function to be minimized is then:

$$M(\hat{x}, \hat{y}) = \sum_{k=1}^{N} \left[d_k - \sqrt{(\hat{x} - x_k)^2 + (\hat{y} - y_k)^2} \right]^2 \tag{2.3}$$

where $\hat{x}$ and $\hat{y}$ are the estimates of the x and y coordinates.

A variation of the steepest descent algorithm is used to find the minimum of a function in an iterative fashion. In this algorithm, unit steps are taken in the direction that minimizes the squared error expressed in (2.2). The gradient ∇M is given by:

$$\nabla M = \begin{bmatrix} \frac{\partial M(\hat{x},\hat{y})}{\partial \hat{x}} \\ \frac{\partial M(\hat{x},\hat{y})}{\partial \hat{y}} \end{bmatrix} \tag{2.4}$$

Differentiating (2.3) with respect to $\hat{x}$ and $\hat{y}$ respectively yields:

$$\frac{\partial M(\hat{x},\hat{y})}{\partial \hat{x}} = -2\sum_{k=1}^{N} \frac{\left| d_k - \sqrt{(\hat{x}-x_k)^2 + (\hat{y}-y_k)^2} \right|}{\sqrt{(\hat{x}-x_k)^2 + (\hat{y}-y_k)^2}} (\hat{x} - x_k) \tag{2.5}$$

$$\frac{\partial M(\hat{x},\hat{y})}{\partial \hat{y}} = -2\sum_{k=1}^{N} \frac{\left| d_k - \sqrt{(\hat{x}-x_k)^2 + (\hat{y}-y_k)^2} \right|}{\sqrt{(\hat{x}-x_k)^2 + (\hat{y}-y_k)^2}} (\hat{y} - y_k) \tag{2.6}$$

The derivatives in (2.5) and (2.6) represent the slope of the surface $M(\hat{x},\hat{y})$ with respect to $\hat{x}$ and $\hat{y}$. Let $\hat{x}$ and $\hat{y}$ in (2.5) and (2.6) be denoted as $\hat{x}_m$ and $\hat{y}_m$ for the m_{th} iteration. The initial guess for the listener location is considered as the average of the beacon locations and is defined as:

$$\hat{x}_{(m=1)} = \sum_{k=1}^{N} \frac{x_k}{N} \tag{2.7}$$

$$\hat{y}_{(m=1)} = \sum_{k=1}^{N} \frac{y_k}{N} \tag{2.8}$$

where N is the number of beacon sensors seen at the present location.

For successive iterations $\hat{x}_m$ and $\hat{y}_m$ are defined as:

$$\hat{x}_m = \hat{x}_{m-1} - s_x \tag{2.9}$$

$$\hat{y}_m = \hat{y}_{m-1} - s_y \tag{2.10}$$

where s_x and s_y are the unit steps taken in x and y respectively, such that:

$$s_x = \frac{dx}{\sqrt{dx^2 + dy^2}} \tag{2.11}$$

$$s_y = \frac{dy}{\sqrt{dx^2 + dy^2}} \tag{2.12}$$

where dx and dy are the directions for the MLE defined as:

$$dx = \frac{\partial M(\hat{x}_{m-1}, \hat{y}_{m-1})}{\partial \hat{x}} \tag{2.13}$$

$$dy = \frac{\partial M(\hat{x}_{m-1}, \hat{y}_{m-1})}{\partial \hat{y}} \tag{2.14}$$

When m reaches a determined maximum number of iterations for the algorithm, a local minimum of the surface $M(\hat{x}, \hat{y})$ is found. This minimum represents the best estimated location of the listener sensor.

The experimental testbed for sensor localization is located on the fifth floor of the six storey Engineering and Computer Science building (ECS) at the University of Victoria. In previous work [35], the beacon sensors were placed mostly on the ceiling on the testing building floor. However, preliminary studies were conducted in [35] on the hearability of the sensors when they were placed on walls. The reason to test the sensors on walls was to find a faster data collection technique. To complete survey data collection of one floor with the beacon sensors on the ceiling could take up to three days. This was due in the most part to the time it requires to place and remove sensors using a ladder [35].

Consequently, it was decided to place the beacon Crickets entirely on walls of the building hallways for this current work. During our test runs, it was found that in some cases the estimated location of the listener exhibited a disproportional error. This error is caused by the existence of outliers in the distance measurements coming from the sensor network. An outlier is an observation that is numerically distant from the rest of the data, so it follows a different distribution. The presence of outliers is

due to NLoS distance measurements, i.e. ultrasound reflections off opposite walls of the hallways in our experimental testbed. Ultrasound reflections were encountered only in hallway-like structures, i.e. two walls separared by a relatively short distance (approximately 160 cm in our testbed). This is also the reason why these reflections did not appear when the Crickets were on the ceiling, since the distance from the ceiling to the ground is larger than 3 m in the tested floors. Fig. 2.1 depicts the wall set-up, where the Crickets were placed along one of the walls to locate the mobile terminal in the hallway. It can be seen that in some cases the Line-of-Sight (LoS) signal reaches the mobile terminal (Cricket 2 and Cricket 3) and in others the NLoS signal is received (Cricket 1).

A set of sensor distance measurements composed of a total of 242 readings collected in a section of a hallway in the fifth floor of the ECS building was analyzed. The distance error for these readings was calculated as the difference between the distance obtained from the sensors and the true distance. Fig. 2.2 displays a histogram of the

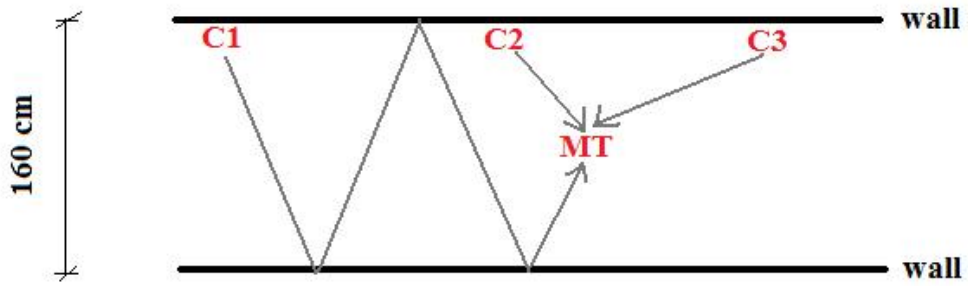

Figure 2.1: Beacon Crickets Wall set-up

distance error. The occurence of outliers can be clearly identified in the right-hand side distribution that is separated from the left-hand side or main distribution of the data. In the next section, a robust window algorithm is introduced to reduce the effect of outliers in the data.

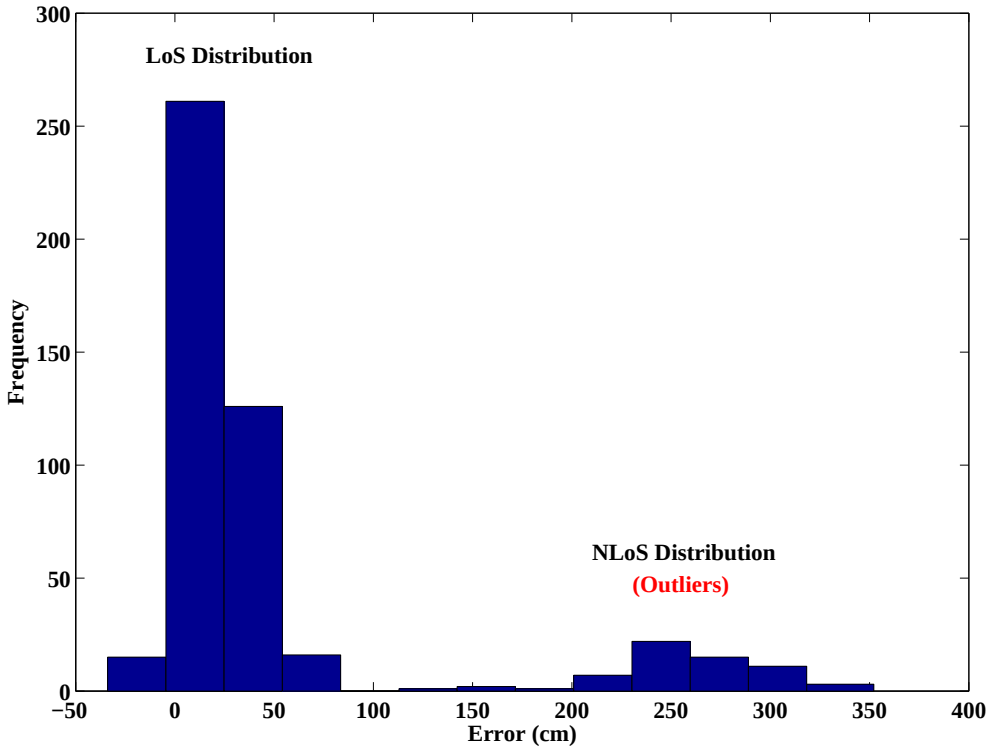

Figure 2.2: Distance Error in listener localization

2.3 Robust Window Function

This section presents a brief overview of robust statistics followed by a description of the conventional Huber Window and its proposed modified version.

2.3.1 Robust Statistics

All classical statistical methods rely explicitly or implicitly on several assumptions that are often not met in practice. The assumption is made that the measurement noise has a Gaussian distribution [47]. However, an assumed normal distribution model, e.g. a localization model with normally distributed residuals, holds only approximately when outliers are found in the data. The existence of outliers and non-Gaussian noise causes many least squares statistical methods to perform poorly, so other techniques are required.

Robust statistics seeks to provide statistical analysis methods that are not unduly affected by outliers or departures from model assumptions in small subsets of the collected data [48]. Robust methods accomplish the task of fitting the bulk of the data well, whether the data contain a small number of outliers or no outliers at all [47]. Several approaches to robust estimation have been proposed, including M-estimators, R-estimators and L-estimators. M-estimators, which are a generalization of MLEs, appear to dominate the field because of their degree of generality and efficiency.

In [49] Robust Statistics is proposed to generalize the MLE as the minimization of:

$$\sum_{k=1}^{N} \rho(m_k) \tag{2.15}$$

where $\rho(\cdot)$ is a positive definite function with a unique minimum at zero and is chosen to increase slower than quadratically. If the argument of $\rho(\cdot)$ is selected, so that, $m_k = d_k - \hat{d}_k(x, y, z)$, the problem of locating the listener using the window function $\rho(m_k)$ can be stated as:

$$(x, y, z) = \arg \min_{(x,y,z)} \sum_{k=1}^{N} \rho \left(d_k - \hat{d}_k(x, y, z) \right) \tag{2.16}$$

The function to be minimized is then:

$$M(\hat{x}, \hat{y}) = \sum_{k=1}^{N} \rho \left(d_k - \sqrt{(\hat{x} - x_k)^2 + (\hat{y} - y_k)^2} \right) \tag{2.17}$$

Differentiating (2.17) with respect to $\hat{x}$ and $\hat{y}$ gives:

$$\frac{\partial M(\hat{x},\hat{y})}{\partial \hat{x}} = -\sum_{k=1}^{N} \frac{\rho'\left(d_k - \sqrt{(\hat{x}-x_k)^2+(\hat{y}-y_k)^2}\right)}{\sqrt{(\hat{x}-x_k)^2+(\hat{y}-y_k)^2}}(\hat{x}-x_k) \tag{2.18}$$

$$\frac{\partial M(\hat{x},\hat{y})}{\partial \hat{y}} = -\sum_{k=1}^{N} \frac{\rho'\left(d_k - \sqrt{(\hat{x}-x_k)^2+(\hat{y}-y_k)^2}\right)}{\sqrt{(\hat{x}-x_k)^2+(\hat{y}-y_k)^2}}(\hat{y}-y_k) \tag{2.19}$$

The derivatives in (2.18) and (2.19) can be used to obtain the best location estimate for the listener similarly as with the MLE.

The minimum points of an objective function are again evaluated by a variation of the steepest descent algorithm. In this case, unit steps are taken in the direction that minimizes the function shown in (2.16). Since the convergence of Robust Statistical methods are more sensitive to an initial guess point for sensor localization, the initial guess is then user defined by clicking on an approximate position on a floor plan in our data collection software.

For successive iterations $\hat{x}_m$ and $\hat{y}_m$, s_x and s_y, and d_x and d_y are defined as in (2.9), (2.10), (2.11), (2.12), (2.13), (2.14) respectively. Similarly as with the MLE, when m reaches a determined maximum number of iterations for the algorithm, the best estimated location of the listener sensor is obtained.

The objective of a robust method is to design a $\psi(m_k)$ function to reduce the influence of outliers by fine-tuning the convergence value of the estimation process, $\hat{\theta} = (\hat{x}_m, \hat{y}_m)$, so that it is the closest possible to θ. Consequently, $\psi(m_k)$ is called the Influence Function (IF).

2.3.2 Conventional Huber Window

The conventional Huber window function is a parabola in the vicinity of zero and increases linearly when $|m| > d$, where m is an error function and d is a tuning

constant used as a cutoff point. In our case, if m is expressed as m_k, the error function for the k_{th} beacon is $m_k = d_k - \hat{d}_k(x, y, z)$ as shown in section 2.3.1. In [49], for the Huber window, the functions $\rho(m_k)$ and $\psi(m_k)$ are given by:

$$\rho(m) = \begin{cases} \frac{m^2}{2} & \text{if } |m| < d \\ d\left(|m| - \frac{d}{2}\right) & \text{if } |m| \geq d \end{cases} \tag{2.20}$$

$$\psi(m) = \begin{cases} m & \text{if } |m| < d \\ d\,\text{sgn}(m) & \text{if } |m| \geq d \end{cases} \tag{2.21}$$

Fig. 2.3 depicts the $\rho(m_k)$ and $\psi(m_k)$ functions. From Fig. 2.3 and Fig. 2.4, and (2.20) and (2.21), it can be clearly seen that most of relevant information lies in the range where $|m| < d$, i.e. when m is within the selected error threshold d. However, in the listener location estimation problem, it was determined that the conventional Huber window function does not performed efficiently since it gives the same weight to all the values of $|m| > d$ and likewise to the values of $|m| < d$. A modification of this window is presented in the next subsection with the intention of overcome this defficiency of the original window.

2.3.3 Modified Huber Window

The conventional Huber Window was modified based on data collected from the sensor network to tailor it to the demands of our specific problem. The goal is to devise an influence function that guarantees convergence of the estimation process at locations where the distance reading from a single Cricket is an outlier and the rest of the distance measurements have a considerably smaller error. Since in the presence of NLoS, the measured distances were approximately 3 times larger than Line-of-Sight (LoS) distances, the outliers always add positively to the measurements, which

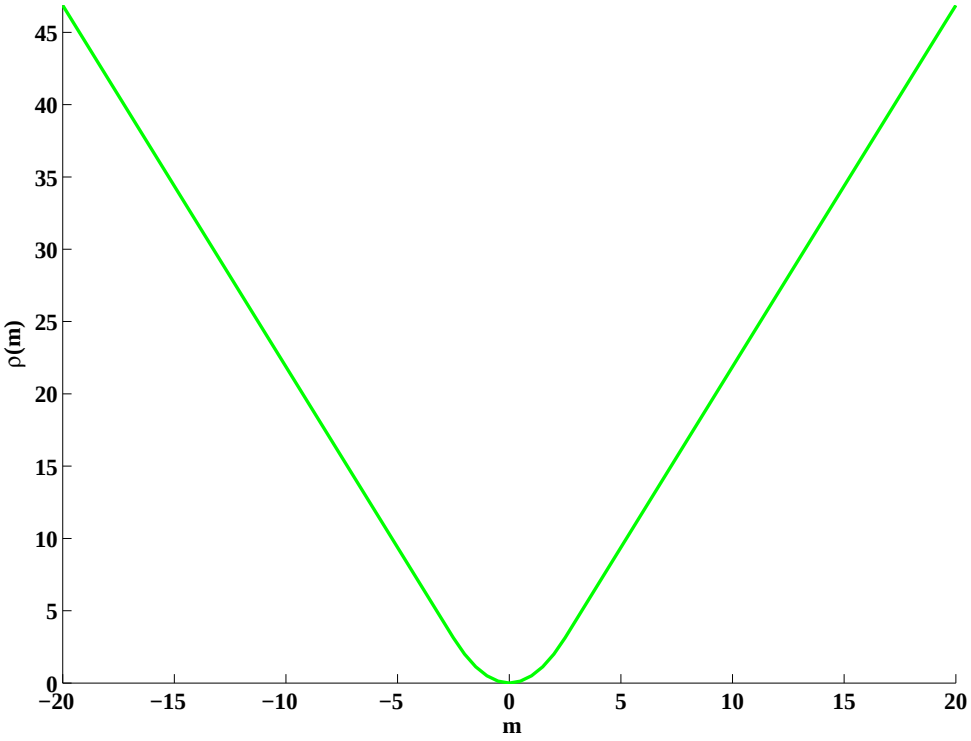

Figure 2.3: ρ function of the Conventional Huber Window

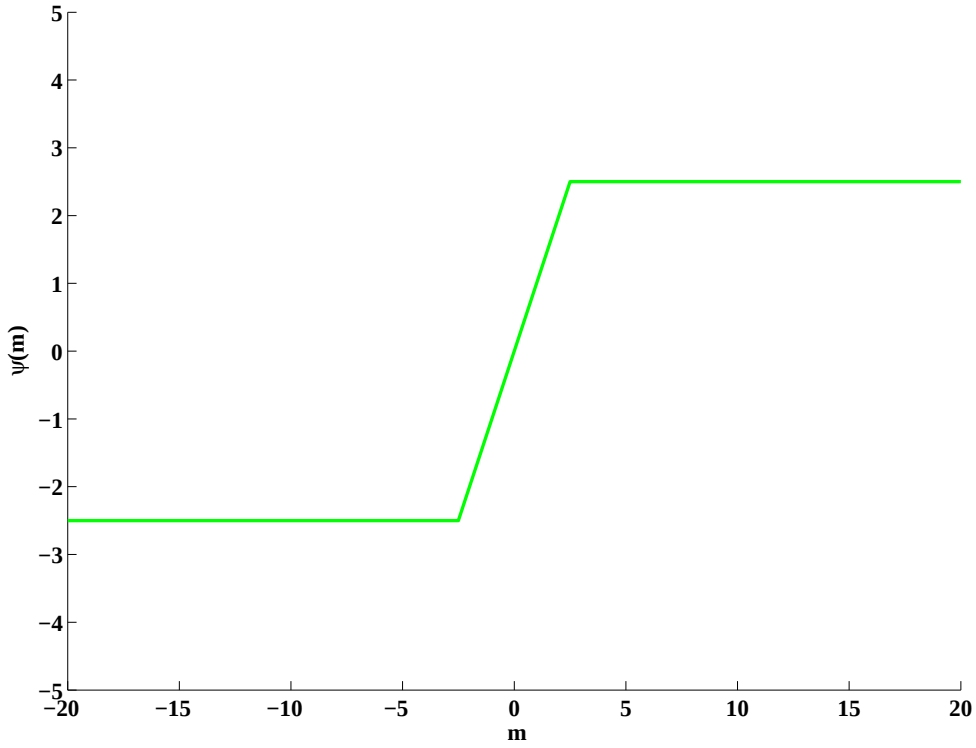

Figure 2.4: ψ function of the Conventional Huber Window

results in an asymmetric influence function. In the Modified Huber Window four intervals were indentified as compared to two in the conventional function and the $\psi(m_k)$ was expressed as:

$$\psi(m) = \begin{cases} m & \text{if } |m| \leq d \\ 2d\,\text{sgn}(m) & \text{if } d < |m| \leq 3d \\ -1.2m^2 & \text{if } m < -d \\ 0.5d\,\text{sgn}(m) & \text{if } |m| > 3d \end{cases} \tag{2.22}$$

In (2.22) d was chosen to be 2.5, since this value is comparable to the distance error in (cm) specified by the manufacturer [46]. In Fig. 2.5, the $\psi(m_k)$ functions of the conventional and modified Huber windows are shown for comparison. In the modified Huber window, the $\psi(m)$ function indicates that less weight was given to negative values of m, i.e. $m < -d$, since $m_k = d_k - \hat{d}_k$, where d_k is the distance measured by the sensors, an NLoS or LoS distance, which is in most cases much larger than $\hat{d}_k$, the estimated distance. The quadratic function in this interval represents a very rapid decrease in the value of the influence function $\psi(m)$ as m becomes more negative and moves further away from the minimum of the function $\rho(m)$ found at $m = 0$.

For $|m| \leq d$, the value of $\psi(m)$ was considered to be the same as that of the original Huber window. The interval in which $|m| \leq d$ is where the most influencial values of m are found since they are the closest to where the minimum of $\rho(m)$ lies (See Fig. 2.3). A linear function was chosen to represent a constant rate of change of the function $\rho(m)$ in the vecinity of the minimum and thus give the values of m in this range the strongest influence in the function $\psi(m)$. The value of $\psi(m)$ for other ranges of m was chosen to reflect more useful information for location estimation in the range of $d < m \leq 3d$ compared to when $m > 3d$. In both cases the influence of m is a constant, but since the range $d < m \leq 3d$ is closer to the minimum of $\rho(m)$

then the values of its influence were selected to be four times larger than the influence values of the range $m > 3d$. The selection of a constant influence for the two intervals when $m > d$ represents a way to prevent the influence from increasing as m becomes larger and moves further away from the minimum of $\rho(m)$.

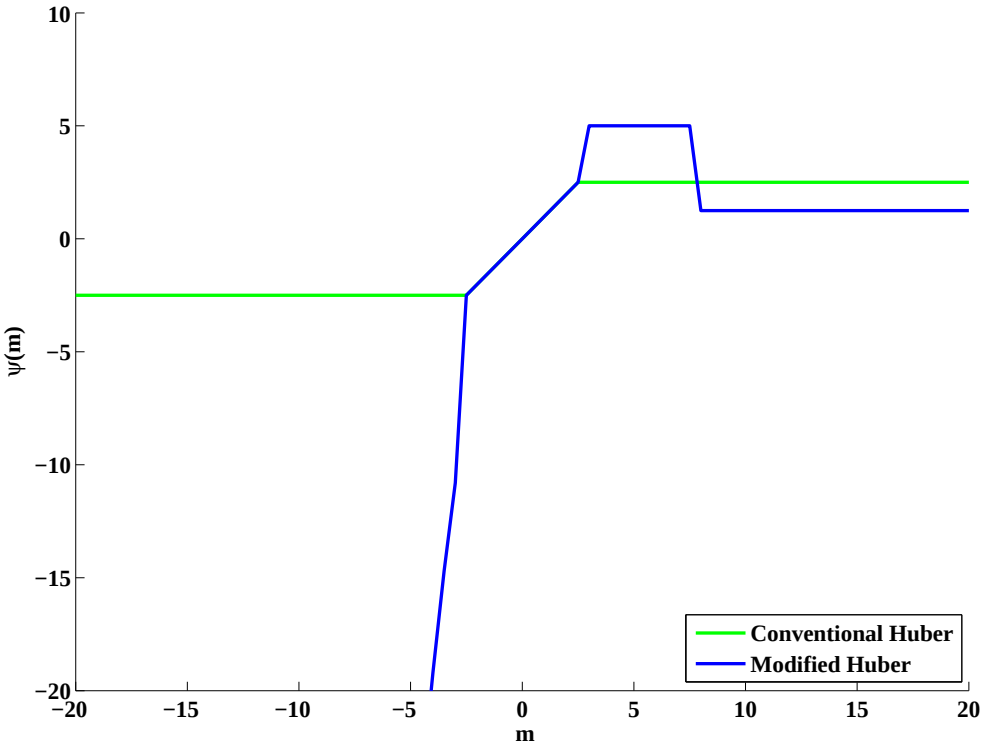

Figure 2.5: ψ functions of the Conventional and Modified Huber Windows

2.4 Robust Cricket Localization

The robustness of the modified Huber window developed in the previous section is tested in the set of distance measurements of Section 2.2. This set was collected along 20 locations with 3 samples at each location, i.e. it contains 60 vectors of distance

measurements. Each vector contains measurements from at least 3 sensors. The error distance for this set was found to be within 10 cm about 85% of the time and had a mean value of 7.4 cm. When localization without a robust method was conducted in this set the error distance was roughly higher than 1 m and when the original Huber window was applied 30 cm. These results demonstrate that the modified Huber window allows the ultrasonic sensors to locate the survey terminal with better accuracy than it is required for radio location.

Chapter 3
Noise Removal

The presence of noise in the RSS measurements of the survey set degrades the localization accuracy and increases the number of survey points required to achieve a desired accuracy; thereby, increasing the cost of survey data collection. Since data collection is labor intensive and expensive, significant efforts need to be expended on finding efficient noise removal techniques to lower the costs of collecting RSS data. A large component of the measurement noise created by multipath propagation is time-invariant over the period of survey data collection [31, 43], i.e. a few hours, if the mobile device is immobile during this period. In an indoor environment, there are radio signal scatterers and reflectors such as furniture and doors which create multipath propagation and are immobile during the period of a data collection session, but are unlikely to all remain in the same position from the time of survey data collection to the time of mobile terminal localization. The effects of these scatterers on the survey measurements is considered as time-invariant measurement noise, but not constant measurement noise, i.e. it changes over a longer period of time, such as days or months. The time-averaging filtering algorithms proposed in previous work will not remove this portion of the noise, so radio location accuracy is still below optimal levels.

The multipath propagation noise that is time invariant over the period of survey collection can be removed by collecting several survey sets at points significantly separated in time, i.e. several hours or days, and then averaging the RSS measurements over the multiple survey sets, but this significantly increases the cost of survey data collection. In this chapter, a detailed description of the Wiener filter and its

application to noise reduction is elaborated to build up the background knowledge for the proposed noise removal technique. The most common filtering method in the literature of noise removal from RSS measurements for indoor radio localization, i.e. time domain filtering, is then presented. Finally, the spatial domain averaging filter is introduced to remove more multipath propagation noise than the previously proposed filtering techniques. The impact of the application of this filter in mobile terminal localization is that the lower level of measurement noise in the survey data creates a substantial accuracy improvement in the localization.

3.1 Wiener Filters

Wiener filters are a class of *linear optimum filters* that play an important role in several applications such as signal restoration, linear prediction, channel equalization and echo cancellation [50, 51]. The original Wiener theory formulated continuous time filters. The extension of the Wiener theory from the continuous time case to the discrete time case is easy and allows implementation on digital hardware or software. In the derivation of the Wiener filter, the Finite Impulse Response (FIR) case will be considered, since it is relatively straightforward to compute and inherently stable [50].

The linear optimum filtering problem to be analyzed is depicted by the block diagram of Fig. 3.1. The filter takes as input a signal $\boldsymbol{y}$ and is characterized by the impulse response or weight vector $\boldsymbol{w}$. The filter produces an output signal denoted $\hat{\boldsymbol{x}}$, where $\hat{\boldsymbol{x}}$ provides an estimate of a desired or target signal $\boldsymbol{x}$. The filter input-output relation is given by:

$$\hat{\boldsymbol{x}} = \boldsymbol{w}^T \boldsymbol{y} \tag{3.1}$$

where $\boldsymbol{y}$ is the input signal and $\boldsymbol{w}^T$ is the Wiener filter coefficient vector. Since the filter input and target signal represent single realizations of jointly wide-sense

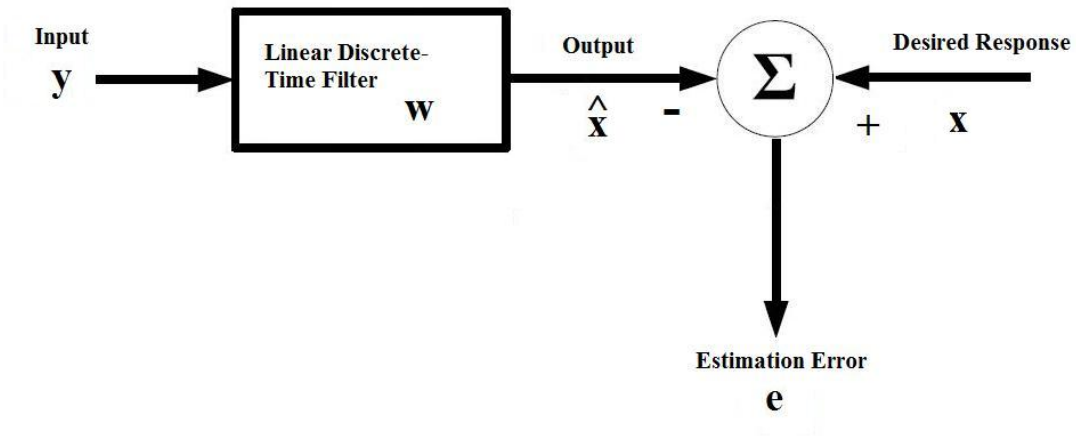

Figure 3.1: Block Diagram Representation of the Linear Optimum Filtering Problem

stationary stochastic processes, both with zero mean, an error with its own statistical characteristics appears in the estimation process [50]. The estimation error $\boldsymbol{e}$ is defined as the difference between the desired signal $\boldsymbol{x}$ and the filter output $\hat{\boldsymbol{x}}$:

$$\begin{aligned} \boldsymbol{e} &= \boldsymbol{x} - \hat{\boldsymbol{x}} \\ &= \boldsymbol{x} - \boldsymbol{w}^T \boldsymbol{y} \end{aligned} \tag{3.2}$$

The objective of the filter is then to make $\boldsymbol{e}$ as small as possible in a statistical sense [50]. In this case the selected criterion for statistical optimization is the minimization of the mean-squared value of the estimation error. Equation (3.2) can be written in a more compact notation as:

$$\boldsymbol{e} = \boldsymbol{x} - \boldsymbol{Y}\boldsymbol{w} \tag{3.3}$$

where $\boldsymbol{e}$ is the error vector, $\boldsymbol{x}$ is the desired signal vector, $\boldsymbol{Y}$ is the input signal matrix, and $\hat{\boldsymbol{x}} = \boldsymbol{Y}\boldsymbol{w}$ is the filter output signal vector. It is assumed that the initial input signal is either known or set to zero [51].

The Wiener filter coefficients are obtained by minimizing the mean-squared error function $\mathrm{E}[\boldsymbol{e}^2]$ with respect to the filter coefficient vector $\boldsymbol{w}$. From equation (3.2), the

mean square estimation error is expressed as:

$$\begin{aligned} \mathrm{E}\left[\boldsymbol{e}^2\right] &= \mathrm{E}[\boldsymbol{x} - \boldsymbol{w}^T\boldsymbol{y}] \\ &= \mathrm{E}[\boldsymbol{x}^2] - 2\boldsymbol{w}^T\,\mathrm{E}[\boldsymbol{y}\boldsymbol{x}] + \boldsymbol{w}^{\boldsymbol{T}}\,\mathrm{E}[\boldsymbol{y}\boldsymbol{y}^T]\boldsymbol{w} \\ &= r_{xx}(0) - 2\boldsymbol{w}^{\boldsymbol{T}}\boldsymbol{r}_{\boldsymbol{yx}} + \boldsymbol{w}^{\boldsymbol{T}}\boldsymbol{R}_{\boldsymbol{yy}}\boldsymbol{w} \end{aligned} \tag{3.4}$$

where $\boldsymbol{R}_{\boldsymbol{yy}} = \mathrm{E}[\boldsymbol{y}\boldsymbol{y}^T]$ is the autocorrelation matrix of the input and $\boldsymbol{r}_{\boldsymbol{xy}} = \mathrm{E}[\boldsymbol{x}\boldsymbol{y}]$ is the cross-correlation vector between the input and the target signals. The gradient of the mean square error function with respect to the filter coefficient vector is obtained from equation (3.4):

$$\begin{aligned} \frac{\partial\,\mathrm{E}[e^2]}{\partial \boldsymbol{w}} &= -2\,\mathrm{E}[\boldsymbol{x}\boldsymbol{y}] + 2\boldsymbol{w}^T\,\mathrm{E}[\boldsymbol{y}\boldsymbol{y}^T] \\ &= -2\boldsymbol{r}_{\boldsymbol{yx}} + 2\boldsymbol{w}^T\boldsymbol{R}_{\boldsymbol{yy}}. \end{aligned} \tag{3.5}$$

The minimum mean square error Wiener filter is obtained by setting equation (3.5) to zero, thus:

$$\boldsymbol{w}^T\boldsymbol{R}_{\boldsymbol{yy}} = \boldsymbol{r}_{\boldsymbol{yx}} \tag{3.6}$$

or equivalently solving for $\boldsymbol{w}$:

$$\boldsymbol{w} = \boldsymbol{R}_{\boldsymbol{yy}}^{-1}\boldsymbol{r}_{\boldsymbol{yx}}. \tag{3.7}$$

The result obtained in equation (3.6) is commonly known as the Wiener-Hopf equation [51].

3.1.1 Analysis of the Error Signal

In order to gain a deeper insight into the operation of Wiener filters an analysis of the variance of the error signal will follow [51]. The Minimum Mean Square Error (MMSE) can be obtained by substituting the Wiener-Hopf equation into equation

(3.4):

$$\begin{aligned} \mathrm{E}\left[\boldsymbol{e}^2\right] &= r_{xx}(0) - \boldsymbol{w}^T \boldsymbol{r}_{\boldsymbol{yx}} \\ &= r_{xx}(0) - \boldsymbol{w}^T \boldsymbol{R}_{\boldsymbol{yy}} \boldsymbol{w}. \end{aligned} \tag{3.8}$$

The term $\boldsymbol{w}^T \boldsymbol{R}_{\boldsymbol{yy}} \boldsymbol{w}$ in equation (3.8) is the variance of the Wiener filter output $\hat{x}$ for zero-mean signals, that is:

$$\sigma_{\hat{\boldsymbol{x}}}^2 = \mathrm{E}[\hat{\boldsymbol{x}}^2] = \boldsymbol{w}^T \boldsymbol{R}_{\boldsymbol{yy}} \boldsymbol{w} \tag{3.9}$$

Equation (3.8) can be then rewritten as:

$$\sigma_{\boldsymbol{e}}^2 = \sigma_{\boldsymbol{x}}^2 - \sigma_{\hat{\boldsymbol{x}}}^2 \tag{3.10}$$

where $\sigma_{\boldsymbol{e}}^2$, $\sigma_{\boldsymbol{x}}^2$, and $\sigma_{\hat{\boldsymbol{x}}}^2$ represent the variances of the error signal, the desired signal and the filter estimate of the desired signal respectively. Generally, the input to the filter $\boldsymbol{y}$ is composed of a signal component $\boldsymbol{x}_s$ and a random noise component $\boldsymbol{n}$:

$$\boldsymbol{y} = \boldsymbol{x}_s + \boldsymbol{n} \tag{3.11}$$

where $\boldsymbol{x}_s$ is the part of the input that is correlated with the desired signal $\boldsymbol{x}$. It is this part that might be converted into the desired signal by the means of a Wiener filter. Substituting equation (3.1) into (3.2) and using equation (3.11), the error can be decomposed into two components as follows:

$$\boldsymbol{e} = \boldsymbol{e}_x + \boldsymbol{e}_n \tag{3.12}$$

The variance of the filter error can be stated as:

$$\sigma_{\boldsymbol{e}}^2 = \sigma_{\boldsymbol{e}_x}^2 - \sigma_{\boldsymbol{e}_n}^2 \tag{3.13}$$

It is important to note that in equation (3.12), $\boldsymbol{e}_x$ is the portion of the signal that cannot be recovered by the filter and represents distortion in the signal output. Similarly, $\boldsymbol{e}_n$ is the portion of the noise that cannot be blocked by the filter [51].

3.1.2 Wiener Filter for Additive Noise Removal

In order to gain an insigth into the operation of the filter, a case study for additive noise reduction is presented. Consider a signal corrupted by additive noise modeled as:

$$\boldsymbol{y} = \boldsymbol{x} + \boldsymbol{n} \tag{3.14}$$

where $\boldsymbol{y}$ is the observed noisy signal, $\boldsymbol{x}$ is the desired noiseless signal and $\boldsymbol{n}$ is the additive noise. Since, the noise-free signal and the noise are uncorrelated, i.e. $\boldsymbol{R_{xn}} = 0$, the autocorrelation matrix of the noisy signal is the sum of the autocorrelation matrix of the noise-free signal and the noise:

$$\boldsymbol{R_{yy}} = \boldsymbol{R_{xx}} + \boldsymbol{R_{nn}}, \tag{3.15}$$

from this derivation it also follows that:

$$\boldsymbol{r_{xy}} = \boldsymbol{r_{xx}} \tag{3.16}$$

where $\boldsymbol{R_{yy}}$, $\boldsymbol{R_{xx}}$ and $\boldsymbol{R_{nn}}$ represent the autocorrelation matrices of the noisy signal, the noiseless signal and the noise respectively, and $\boldsymbol{r_{xy}}$ is the cross-correlation vector of the noiseless signal and the noisy signal. Substituting (3.15) and (3.16) into (3.7) yields:

$$\boldsymbol{w} = \left(\boldsymbol{R_{xx}} + \boldsymbol{R_{nn}}\right)^{-1} \boldsymbol{r_{xx}} \tag{3.17}$$

Equation (3.17) is the optimal linear filter for additive noise removal.

3.2 Time Domain Averaging for Noise Removal

For a location, $\boldsymbol{\theta}$, the random vector of noisy RSS measurements for time t, $\boldsymbol{V}(\boldsymbol{\theta}, t)$, is composed of a deterministic portion that is a function only of location, $\bar{\boldsymbol{v}}(\boldsymbol{\theta})$, and an additive random portion that is a function of both location and time, $\boldsymbol{N}(\boldsymbol{\theta}, t)$, so that:

$$\boldsymbol{V}(\boldsymbol{\theta}, t) = \bar{\boldsymbol{v}}(\boldsymbol{\theta}) + \boldsymbol{N}(\boldsymbol{\theta}, t). \tag{3.18}$$

The noise process is further decomposed as:

$$\boldsymbol{N}(\boldsymbol{\theta}, t) = \boldsymbol{N}(\boldsymbol{\theta}) + \boldsymbol{N}(t) \tag{3.19}$$

where $\boldsymbol{N}(t)$ is a random noise process that varies over time, and $\boldsymbol{N}(\boldsymbol{\theta})$ is a random noise process over location.

Since $\bar{\boldsymbol{v}}(\boldsymbol{\theta})$ is deterministic, the variations of the RSS are caused by the noise process $\boldsymbol{N}(\boldsymbol{\theta}, t)$. The reduction of the time-varying noise $\boldsymbol{N}(t)$ has been well studied with the use of the average or median filter [38], [39], [40], [41], [42]. Based on the work presented in [38], the vector of RSS measurements at a fixed location can be seen as:

$$\boldsymbol{V}(t) = \bar{\boldsymbol{v}} + \boldsymbol{N}(t). \tag{3.20}$$

where $\boldsymbol{V}(t)$ represents the random RSS vector that varies with time only.

The median filter consists of applying an average process to the temporal trajectory of the RSS to reduce $\boldsymbol{N}(t)$. At a fixed location, $\boldsymbol{N}(t)$ represents short-term variations in the RSS due to fast fading [39]. Thus, in [40] the filter is regarded as:

$$\tilde{\boldsymbol{V}}(t) = \text{median}\left\{\boldsymbol{V}(\tau) | t - T_s < \tau \leq t\right\} \tag{3.21}$$

where T_s is the time interval for the median filter.

In [40] a study of the impact of the size of the time interval for the median filter is presented. Two cases were analyzed: $T_s = 30$ and 120 s. It was shown that the average filter produced more stable RSS values when $T_s = 120$ s and that the location estimates exhibited a larger variance when $T_s = 30$ s. The mean and the standard deviation of the localization errors for sets of T_s and the packet transmision rate were also calculated. Their results show that as the rate and T_s increase, the mean and the standard deviation of the error decrease.

Ref. [38] presents a autoregresive model that uses the average of samples from the same WAP. It was shown that the autocorrelation of consecutive RSS samples from

the same WAP can have values as high as 0.9. Consequently, it was demonstrated that when this high autocorrelation was taken into consideration, the localization accuracy improved by 50%. Both [38] and [40] concluded that the value of T_s represents a tradeoff between the localization accuracy and the latency of the location system.

In [39] a median of a set of 5 measurements separated by 250 ms was used as the optimal RSS measurement to reduce the variations caused by fast fading. It was shown that when the median filter was used the RSS variance was less than the variance produced by shadowing effects in the environment. Finally, another time domain noise reduction technique is introduced in [42]. This technique is based on Singular Value Decomposition (SVD). A Hankel-form matrix, i.e. a matrix where the elements $a_{i,j} = a_{i-1,j+1}$, obtained from RSS of available WAPs is decomposed into two orthogonal subspaces: signal and noise via diagonalization. The noise subspace is suppressed and the RSS measurements are reconstructed from the signal subspace only.

Following the analysis in [38], an average process is applied to $\boldsymbol{V}(t)$. t will be replaced by n as a time index for the discrete time case, such that:

$$\mathrm{A}[\boldsymbol{V}(n)] = \frac{1}{N}\sum_{n=0}^{N-1}\boldsymbol{V}(n) \tag{3.22}$$

where A[·] is the average process and N is the length of the time sequence.

The variance of A is calculated as:

$$\begin{aligned}\mathrm{Var}\left(\mathrm{A}[\boldsymbol{V}(n)]\right) &= \mathrm{Var}\left(\mathrm{A}\left[\bar{\boldsymbol{v}} + \boldsymbol{N}(n)\right]\right)\\ &= \mathrm{Var}\left(\mathrm{A}\left[\boldsymbol{N}(n)\right]\right)\\ &= \frac{1}{N}\mathrm{Var}\left(\boldsymbol{N}(n)\right)\end{aligned} \tag{3.23}$$

Equation (3.23) demonstrates that the lower the variance of $\boldsymbol{V}(n)$ at each location, the better the ability of the system to discriminate distinct locations and the higher the accuracy.

3.3 Spatial Domain Averaging for Noise Removal

Despite the efforts to reduce $\boldsymbol{N}(t)$, averaging measurements collected at a single location over time will not reduce $\boldsymbol{N}(\boldsymbol{\theta})$, which is the noise produced by the multipath propagation effect. Decreasing the effect of $\boldsymbol{N}(\theta)$ is highly relevant in WLAN terminal localization since a sizeable contribution of the noise varies only with spatial movement. In this section, a discrete Wiener filter is developed to reduce the measurement noise levels caused by multipath propagation. The objective of the noise reduction technique developed in this thesis is to decrease $\boldsymbol{N}(\boldsymbol{\theta})$ in the RSS measurements in the survey set using spatial averaging.

Key to the design of the spatial domain averaging algorithm and the estimator is the assumption that the terminal locations, $\boldsymbol{\theta}$, are samples of a random vector $\boldsymbol{\Theta}$ and the measured RSS vectors, $\boldsymbol{v}$, are samples of the random vector $\boldsymbol{V}$ which have the joint PDF of terminal locations and measurements denoted as $\mathrm{f}_{\boldsymbol{\Theta},\boldsymbol{V}}(\boldsymbol{\theta},\boldsymbol{v})$. Ideal time filtering is assumed so the measurement equation (3.18) can be rewritten as:

$$\boldsymbol{V}(\boldsymbol{\theta}) = \bar{\boldsymbol{v}}(\boldsymbol{\theta}) + \boldsymbol{N}(\boldsymbol{\theta}). \tag{3.24}$$

where all time-variant noise is assumed to have been completely removed. The measured survey RSS for location $\boldsymbol{\theta_k}$ is one sample value of the random vector $\boldsymbol{V}(\boldsymbol{\theta_k})$. The objective of noise removal is to obtain an estimate of $\bar{\boldsymbol{v}}(\boldsymbol{\theta_k})$ for k = 1, ...,N from the noisy measurements v_k.

Noise reduction is performed for the RSS measurements for each WAP independently. For the i^{th} WAP, a random vector $\tilde{\boldsymbol{V}}_i$ is defined with the k_{th} entry, $\tilde{\boldsymbol{V}}_i[k]$, being the measured RSS signal at survey location k, $\boldsymbol{\theta}_k$ for WAP i, so $\tilde{\boldsymbol{V}}_i[k]$ is the i_{th} entry of the random vector $\boldsymbol{V}(\boldsymbol{\theta_k})$. The measured survey data for the i^{th} WAP, $\tilde{\boldsymbol{v}}_i$, is one sample vector of the random vector $\tilde{\boldsymbol{V}}_i$. This vector is modelled as the sum of two processes: $\tilde{\boldsymbol{\delta}}_i$, which is the deterministic RSS signal for radio location created by immobile features in the network area, and $\tilde{\boldsymbol{N}}_i$ which is the measurement noise not

useful for radio location. The k_{th} entry of $\tilde{\hat{\boldsymbol{v}}}_i$ is equal to the $i_t h$ entry of $\bar{\boldsymbol{v}}(\boldsymbol{\theta_k})$.

$\tilde{\boldsymbol{N}}_i$ reflects the influence of furniture, shadowing effects, and the opening and closing of doors on the RSS in the network environment. $\tilde{\boldsymbol{N}}_i$ is time-invariant over the measurement period when the survey data is measured at $\boldsymbol{\theta}_i$, but it is unlikely to have the identical value when a mobile terminal moves to this position during radio location. The RSS measurement model for the i^{th} WAP is given by:

$$\tilde{\boldsymbol{V}}_i = \tilde{\hat{\boldsymbol{v}}}_i + \tilde{\boldsymbol{N}}_i. \tag{3.25}$$

A discrete filter matrix, $\boldsymbol{W}$, is derived so that noise reduced measurements for the $i_t h$ WAP are calculated based on (3.1) with:

$$\tilde{\hat{\boldsymbol{V}}}_i = \boldsymbol{W}^T \tilde{\boldsymbol{V}}_i \approx \tilde{\hat{\boldsymbol{v}}}_i. \tag{3.26}$$

The method proposed in this thesis is to use a Wiener-Hopf formulation of $\boldsymbol{W}$ (Equation (3.7)). It is assumed that the measurement noise vector is independent of $\tilde{\hat{\boldsymbol{v}}}_i$ so the Wiener-Hopf solution for $\boldsymbol{W}$ is given by:

$$\boldsymbol{W} = \left[\mathrm{Cov}\left(\hat{\boldsymbol{V}}_i\right)\right]^{-1} \mathrm{Cov}\left(\tilde{\hat{\boldsymbol{v}}}_i\right) \tag{3.27}$$

where $\mathrm{Cov}(\cdot)$ is the covariance operator [50], [51]. In (3.27), $\tilde{\hat{\boldsymbol{v}}}_i$ is treated as a random vector.

The covariance matrix of $\boldsymbol{M}_i$ is assumed to be exponential with respect to separation distance of two points, so that if $\boldsymbol{C}^i_{MM}[j,k]$ refers to the k^{th} entry of the j^{th} row of $\mathrm{Cov}(\tilde{\hat{\boldsymbol{v}}}_i)$ then:

$$\boldsymbol{C}^i_{MM}[j,k] = \exp\left(-\frac{|\boldsymbol{\theta}_j - \boldsymbol{\theta}_k|}{d}\right) \tag{3.28}$$

where d is a correlation distance constant. Exponential correlation of RSS signals is often used for shadow fading in outdoor locations [52]. The optimal correlation for indoor locations is not known but it will be shown in Section 4.2 that the correlation

in (3.28) provides excellent noise removal performance. The noise is assumed to be identically distributed and independent for each survey point measurement, so that:

$$\mathrm{Cov}\left(\tilde{\boldsymbol{V}}_i\right) = \boldsymbol{C}^i_{MM} + \sigma^2 \boldsymbol{I} \tag{3.29}$$

where σ^2 is the mean noise power for each survey RSS measurement normalized to the mean squared value of the deterministic portion of the RSS and $\boldsymbol{I}$ is an appropriately sized identity matrix. To remove noise from the measurements, the covariances calculated from (3.28) and (3.29) are substituted into (3.27) to obtain $\boldsymbol{W}$, which is then applied as demonstrated in (3.26) to the vector of RSS measurements for each WAP. The noise removal is performed on a given survey set once and the noise reduced survey set is then used for radio location. Thus, the cost of online radio location is not increased.

In Section 4.2, the results of this noise removal are presented and compared with the use of uniform survey point collection. It is known that noise removal works better if the correlation of the components of the RSS signals $\tilde{\hat{\boldsymbol{v}}}_i$ is higher; i.e. the noise reduction is more efficient for a given survey point if many other survey points are located in close proximity. If survey points are spread uniformly over a network area, the noise removal for the RSS signal of each point will work less effectively than if survey points are clustered together. It will be demonstrated in the same section, that clustering points for better noise removal provides substantial gains in location accuracy.

Chapter 4

WLAN Terminal Localization with Spatial Filtering

This chapter describes how the spatially filtered survey RSS measurements are used to create an accurate WLAN location fingerprinting system. A Minimum Mean Square Error (MMSE) estimator that uses an approximate joint PDF of RSS measurements and location information from survey data is suggested for terminal localization. As mentioned in Section 1.1, locations in the survey set that have the same hearability of WAPs as the current location in the test set will form a subset of measurements. This selection method must be consistent from the data collection phase and the localization phase or otherwise an undesired bias is created [53]. A typical selection method is to choose those m WAPs belonging to a publicly maintained network that have the highest RSS viewed by the mobile device. All survey points that have visibility to these m WAPs comprise the subset of survey points used for localization. In the following subsection, a kernel or Parzen Window Estimator is presented to implicitly characterize the RSS-position relation in a WLAN environment.

4.1 Parzen Window Estimator

The Parzen Window Estimator is an approximation of the MMSE estimator. The Mean Square Error (MSE) of the mobile terminal localization is defined as:

$$\text{MSE} = \text{E}\left\{\left|\hat{\boldsymbol{\theta}}(\boldsymbol{v}) - \boldsymbol{\Theta}\right|^2\right\} \tag{4.1}$$

where $|\cdot|$ is the Euclidean length operator used as the criterion to determine the quality of our localizations. The MMSE which minimizes the expected MSE estimator

is known to be $\hat{\boldsymbol{\theta}}_{MMSE}(\boldsymbol{v}) = \mathrm{E}\left[\boldsymbol{\Theta}|\boldsymbol{V}=\boldsymbol{v}\right]$, where $\mathrm{E}\left[\boldsymbol{\cdot}|\boldsymbol{V}=\boldsymbol{v}\right]$ denotes the expectation operator conditioned on the measured RSS vector taking the value $\boldsymbol{V}=\boldsymbol{v}$ [34]. The MMSE can be expanded as:

$$\begin{aligned}\hat{\boldsymbol{\theta}}_{MMSE}(\boldsymbol{v}) &= \int_{\boldsymbol{S}} \boldsymbol{\theta} \mathrm{f}_{\boldsymbol{\Theta}}\left(\boldsymbol{\theta}|\boldsymbol{V}=\boldsymbol{v}\right) \mathrm{d}\boldsymbol{\theta} \\ &= \frac{\int_{\boldsymbol{S}} \boldsymbol{\theta} \mathrm{f}_{\boldsymbol{\Theta},\boldsymbol{V}}(\boldsymbol{\theta},\boldsymbol{v}) \mathrm{d}\boldsymbol{\theta}}{\int_{\boldsymbol{S}} \mathrm{f}_{\boldsymbol{\Theta},\boldsymbol{V}}(\boldsymbol{\theta},\boldsymbol{v}) \mathrm{d}\boldsymbol{\theta}}\end{aligned} \tag{4.2}$$

where S is the region where the mobile device is known to reside determined by the measuring WAP selection procedure [34], [54]. A direct application of (4.2) for localization poses the problem of knowing the joint PDF, $\mathrm{f}_{\boldsymbol{\Theta},\boldsymbol{V}}(\boldsymbol{\theta},\boldsymbol{v})$ of locations, $\boldsymbol{\Theta}$, and RSS measurements, $\boldsymbol{V}$. This problem is circumvented by using a Parzen window technique to approximate the joint PDF as a sum of kernel functions with each kernel function centered on the joint location vector and RSS measurement vector for each survey point [55], [56], [57]. The approximate joint PDF of terminal locations and RSS measurements based on survey data using the Parzen window technique is expressed as:

$$\mathrm{f}_{\boldsymbol{\Theta},\boldsymbol{V}}(\boldsymbol{\theta},\boldsymbol{v}) = \frac{(h_v)^{-L}(h_\theta)^{-3}}{N} \sum_{i=1}^{N} \mathrm{K}_v\left(\frac{\boldsymbol{v}-\boldsymbol{v}_i}{h_v}\right) \mathrm{K}_\theta\left(\frac{\boldsymbol{\theta}-\boldsymbol{\theta}_i}{h_\theta}\right) \tag{4.3}$$

where $\mathrm{K}_v(\cdot)$ is the kernel function for RSS measurements, K_θ is the kernel function of terminal locations, N is the number of survey points, and L is the number of RSS measurements in each measurement vector. The constants h_v and h_θ are smoothing parameters known as kernel widths, which characterize the propagation and location environments. Standard multivariate Gaussian density functions are used for the kernel functions:

$$\mathrm{K}_v(\boldsymbol{v}) = (2\pi)^{-L/2} \exp\left(-\frac{\boldsymbol{v}^T\boldsymbol{v}}{2}\right) \tag{4.4}$$

$$\mathrm{K}_\theta(\boldsymbol{\theta}) = (2\pi)^{-3/2} \exp\left(-\frac{\boldsymbol{\theta}^T\boldsymbol{\theta}}{2}\right) \tag{4.5}$$

Using the properties of the first and second moments of a Gaussian random vector to substitute (4.4) and (4.5) into (4.3) and compute the integrals in (4.2). The mobile terminal localization is then:

$$\hat{\boldsymbol{\theta}}(\boldsymbol{v}) = \sum_{i=1}^{N} w_i(\boldsymbol{v})\boldsymbol{\theta}_i, \tag{4.6}$$

with the weight $w_i(\boldsymbol{v})$ for each survey point being given by:

$$w_i(\boldsymbol{v}) = \frac{\mathrm{K}_v(\frac{\boldsymbol{v}-\boldsymbol{v}_i}{h_v})}{\sum_{j=1}^{N} \mathrm{K}_v(\frac{\boldsymbol{v}-\boldsymbol{v}_j}{h_v})} \tag{4.7}$$

The accuracy of the localization procedure is a function of the noise removal algorithm parameters d and σ^2 and the estimation algorithm parameter $P = \{h_v\}$. The technique to calculate the optimal parameter P for radio location accuracy uses two independent datasets A and B of RSS measurements collected at known locations. Dataset A is used as the survey set, whereas dataset B is used as the validation set. The location of each data collection point in dataset B is estimated using the Parzen window estimator in (4.6) using survey set A for a given h_v. The MSE of the localization error is computed while varying the parameter h_v. The value of h_v that produces the minimum MSE is then used as the kernel width. If the sample locations for dataset B are drawn from the same density $\mathrm{f}_{\boldsymbol{\Theta}}(\boldsymbol{\theta})$ as the PDF of terminal locations then value of h_v that minimizes the MSE for dataset B will approach the optimal value as the size of dataset B goes to infinity. In practice, only finite size data sets may be used, so sub-optimal calculations of h_v are performed.

Due to high costs and time consumption associated with collecting multiple datasets, it is convenient to determine the optimal kernel width h_v using only the survey dataset via a so-called cross-validation technique [58]. Cross-validation entails removing one point from the survey set and then localizing that survey point using the rest of the survey points and their respective RSS measurement vectors. The location estimation error for that particular survey point is then computed. This process is iterated for

all the points in the survey set and the cross-validation MSE value is obtained. For a suitably large survey set, the h_v value that produces the minimum cross-validation MSE is approximately equal to the optimal kernel width. The cross-validation MSE is given by:

$$\mathrm{MSE}_{cross} = \sum_{i=1}^{N} \left| \boldsymbol{\theta}_i - \sum_{k=1,\neq i}^{N} \boldsymbol{\theta}_k \tilde{w}_k^i(\boldsymbol{v}_i) \right|^2 \tag{4.8}$$

where a modified version of the weight function from (4.7) is obtained:

$$\tilde{w}_k^i(\boldsymbol{v}_i) = \frac{\mathrm{K}_v(\frac{\boldsymbol{v}_i - \boldsymbol{v}_k}{h_v})}{\sum_{j=1,\neq i}^{N} \mathrm{K}_v(\frac{\boldsymbol{v}_i - \boldsymbol{v}_j}{h_v})} \tag{4.9}$$

4.2 Localization Accuracy with Spatial Filtering

The experimental testbed for radio location with noise removal is located on the fifth and sixth floors of the ECS. The experiments were conducted in public conference rooms and hallways. This testbed is the same that was used in previous work; thus, for a more detailed description the reader is referred to [53]. The survey database of the ECS sixth floor includes 261 survey point locations, while the survey database of the ECS fifth floor contains 200 survey point locations. For all surveyed points on both floors, more than 35 unique WAPs from the university WLAN were visible to the mobile terminal, with a minimum of 12 WAPs being visible at all survey points. The localization process was performed with measurements from 11 WAPs for the 6th floor and from 10 WAPs for the 5th floor.

To perform radio location and noise removal effectively, it is necessary to use proper values of the estimation algorithm parameter $P = \{h_v\}$; and the noise removal parameters d, and σ^2. In order to obtain these values, the cross-validation method presented in Section 4.1 is used. The optimization strategy was to first find the ranges of d and σ^2 that yielded the best noise reduction results. Fine search spaces have been found experimentally to be $0.25 \leq d \leq 1.50$ metres and $0 \leq \sigma^2 < 1$. Then the best

range of values for the estimation parameter was determined based on the localization accuracy produced when the noise reduced survey set with $0.25 \leq d \leq 1.50$ metres and $0 \leq \sigma^2 < 1$ was used. Experimentally the most suitable range for h was found to be $0.1 \leq h_v \leq 6.0$. This search may be time consuming but it is performed offline and only needs to be performed once for a given survey set. As a result, the computational cost of each localization is not increased.

The parameter values obtained from the cross-validation process were used for noise removal and then localization was performed on an independent dataset of over 400 points for each floor to evaluate the location accuracy. The test sets are collected on multiple days with the minimum time between survey set and data set collection being two weeks with some dataset points collected up to three months after the survey set data collection. The test sets locations are uniformly distributed over the public areas on each floor. In order to determine the best distribution of survey points for a survey set, two point sets were used as survey sets and the resulting localization accuracy compared. In the first set, the location points were collected in a uniform straight-line fashion. In the second set, the locations were collected in clusters of four points. The point locations for each type of survey set for the fifth floor are plotted in Fig. 4.1 and Fig. 4.2. The uniform survey set contains 215 points spaced at 70 cm apart. The clustered survey set has 208 points. Points inside of a cluster are spaced at 60 to 70 cm apart and the approximate distance between clusters is 120 cm. In both cases, the RSS values were averaged for 30 seconds at each survey point to remove time-varying noise. To show the advantage of the noise removal, radio location was also performed on a survey set which had only time filtering noise removal performed on it.

The results of the radio location experiments are summarized in Table 4.1. It can be seen that the time averaging noise removal technique provides an improvement in radio location accuracy. This improvement is about 16% (193 cm from 229 cm)

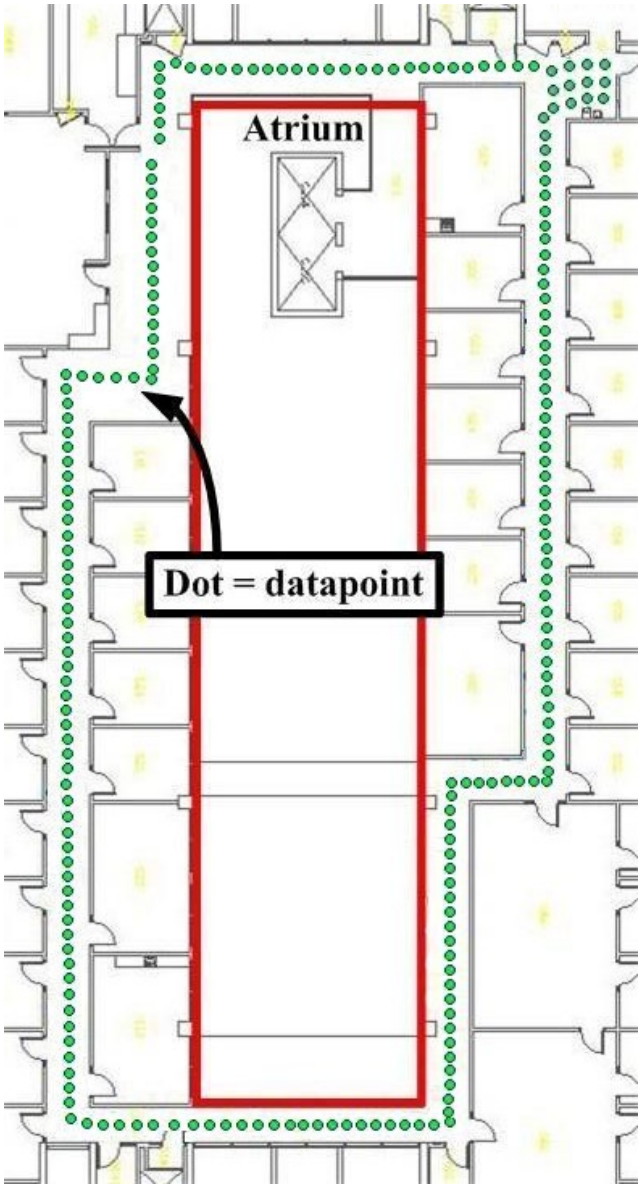

Figure 4.1: Uniform Survey Set

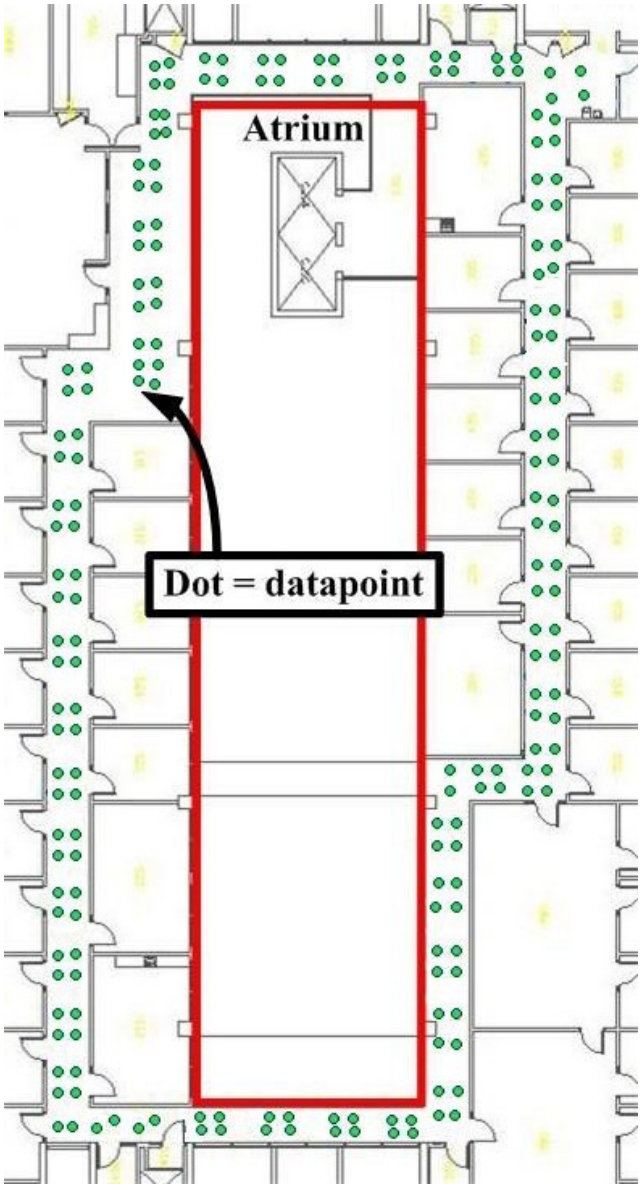

Figure 4.2: Clustered Survey Set

when using the clustered survey set on the fifth floor and 11% (248 cm from 280 cm) on the sixth floor. It is also noted that the clustered survey set provides accuracy improvements to the uniform set even when no spatial averaging is performed. This is because the Parzen window estimator includes some spatial averaging already by from the weighted averaging performed in the location estimate calculations. The lower accuracy on the sixth floor is due to the presence of large meeting rooms in the test area. Large open spaces like this generate less significant RSS features compared to hallways so the accuracy of pattern recognition based radio location is lower in these areas. The test sets points are uniformly distributed over the floor so the uniform survey set points are a better match to the test sets point distributions, the gain in accuracy for the clustered survey set is provided by the superior noise removal.

Table 4.1: Radio Location Summary for Noise Removal

	Normal Survey Set		**Filtered Survey Set**			
	h_v	RMSE	h_v	d	σ^2	RMSE
Fifth Floor Uniform Survey	4.3	251 cm	3.6	1000 cm	0.28	236 cm
Fifth Floor Clustered Survey	5.1	229 cm	3.5	550 cm	0.2	193 cm
Sixth Floor Clustered Survey	3.2	280 cm	3.4	850 cm	0.24	248 cm

A more thorough comparison of radio location accuracy for the fifth floor is obtained from the plot of the Cumulative Distribution Function (CDF) of the distance between the true terminal location and the estimated terminal location in Fig. 4.3. This plot shows the probability that the distance error is below the specified value on the x-axis. This plot also shows that the estimated location is within 400 cm of the true location for the noise-reduced clustered survey set about 90% of the time

but without the noise reduction the distance increases to 450 cm and this distance is 500 cm for the uniform survey set. It is evidently seen that the spatial domain filter improves the localization accuracy. It is also seen that survey points in clusters provide superior accuracy compared to a uniform distributed survey set locations.

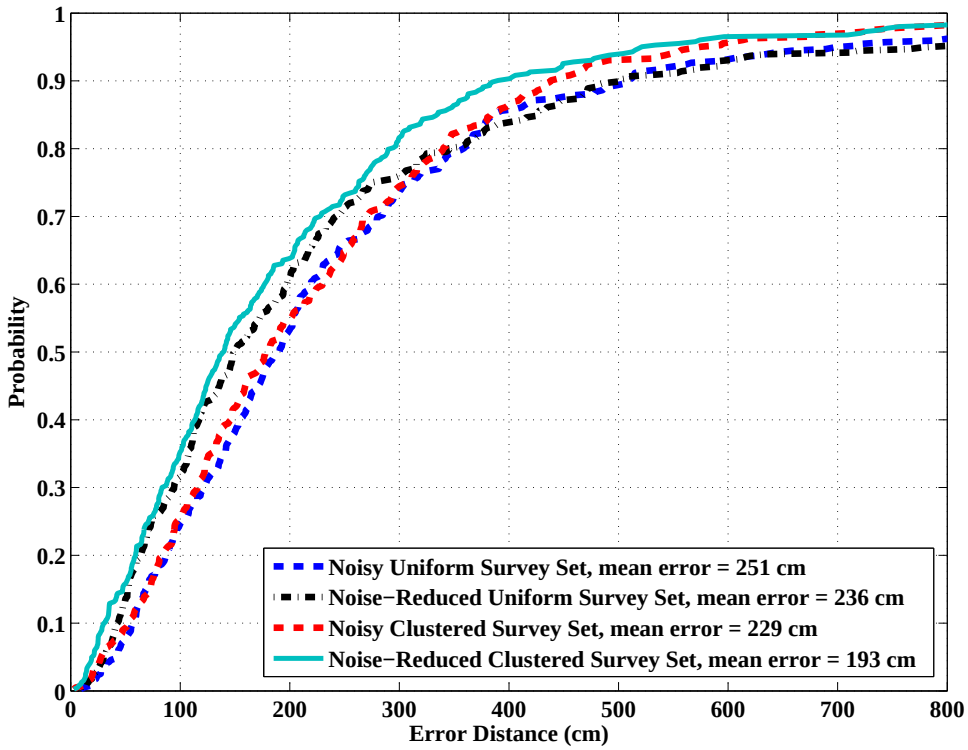

Figure 4.3: Location Accuracy Comparison

4.3 Conclusion

A spatial-averaging noise removal filter that decreases the effect of multipath propagation noise on the survey RSS measurements collected for indoor radio location purposes has been presented. Noise reduction for two distinct geometries used in

data collection of survey points was examined. The results show that the location accuracy improved by 16% when the noise reduction filter is used. Additionally, these results indicate that survey data collection in clusters of points allow a survey set to better characterize the RSS in an indoor environment when the spatial-averaging noise removal filter is used.

Chapter 5

Calibration for Handset Localization

Several studies [32], [33], [44] have suggested that RSS measurements with distinct types of wireless cards can be significantly different. Some vendors manufacture better receivers for WLAN cards than others. The way of measuring the RF energy can also vary from one kind of card to another. For example, Cisco's 802.11 card has a maximum RSSI value based on 100 levels, whereas the Atheros chipset has a maximum of 60 levels [32]. For localization purposes, a finer granularity will help the system better differentiate between two locations. The RSS value range and the standard deviation of the RSS are more relevant indicators for a localization system as opposed to a higher average RSS at a particular position considered better for communication tasks [32]. Furthermore, the number of antennas, the diversity schemes employed and the orientation of a devices can also cause substantial differences in the RSS levels from various mobile terminals.

The problems exposed above can be noticed when different mobile devices are used in the data colection phase and the location estimation phase. The raw RSS measurements from these two devices can produce a disproportional error when they are used for localization. For instance, RSS measurements collected with a laptop computer have a noticeable variability from RSS data collected with portable handsets. This variation might be caused by several factors such as that modern laptops have two Wi-Fi antennas and most of mobile handsets only one, that Wi-Fi antennas in laptops are usually found near the LCD screen whereas the position of antennas in handsets vary between several devices [59], and even the effect of body shadowing of the user. Thus, it is imperative to develop a calibration method that brings the RSS

measurements in the data set to a level comparable to the RSS measurements in the survey set and might eventually be useful for handling handset orientation and the body shadowing effect. In this thesis, a calibration method via an affine transformation between RSS values from one mobile terminal to another is introduced.

The best set of parameters for the affine trasformation can be found offline making use of the two sets of RSS measurements. However, this requires to have two complete sets collected. Thus, when more than two devices are involved in a localization process, it becomes time consuming and labor intensive to collect an entire RSS measurement set for every mobile terminal to determine the transformation parameters. Consequently, an online automated method to find these parameters is proposed in this thesis as an inexpensive and rapid way to match the signal levels from several mobile devices. A key element of this automated calibration method is the estimation of the RSS measurements of the data set based on the locations of the mobile terminal.

5.1 RSS Estimation

The estimation of the RSS measurements based on the locations of the mobile device is the reverse process as the one described in Section 4.1. The MSE of the RSS measurements is given by:

$$\text{MSE} = \text{E}\left\{|\hat{\boldsymbol{v}}(\boldsymbol{\theta}) - \boldsymbol{V}|^2\right\}. \tag{5.1}$$

The MMSE which minimizes the expected MSE estimator is $\hat{\boldsymbol{v}}_{MMSE}(\boldsymbol{\theta}) = \text{E}\left[\boldsymbol{V}|\boldsymbol{\Theta} = \boldsymbol{\theta}\right]$, where $\text{E}\left[\cdot|\boldsymbol{\Theta} = \boldsymbol{\theta}\right]$ denotes the expectation operator conditioned on the location vector

taking the value $\boldsymbol{\Theta} = \boldsymbol{\theta}$. The MMSE is then expanded as:

$$\begin{aligned}\hat{\boldsymbol{v}}_{MMSE}(\boldsymbol{\theta}) &= \int_{\boldsymbol{S}} \boldsymbol{v} \mathrm{f}_{\boldsymbol{V}}\left(\boldsymbol{v}|\boldsymbol{\Theta} = \boldsymbol{\theta}\right) \mathrm{d}\boldsymbol{v} \\ &= \frac{\int_{\boldsymbol{S}} \boldsymbol{v} \mathrm{f}_{\boldsymbol{\Theta},\boldsymbol{V}}(\boldsymbol{\theta}, \boldsymbol{v}) \mathrm{d}\boldsymbol{v}}{\int_{\boldsymbol{S}} \mathrm{f}_{\boldsymbol{\Theta},\boldsymbol{V}}(\boldsymbol{\theta}, \boldsymbol{v}) \mathrm{d}\boldsymbol{v}}. \end{aligned} \tag{5.2}$$

In a similar analysis as exposed in Section 4.1, substituting (4.4) and (4.5) in (4.3) and performing the integrations in (5.2), the RSS estimation procedure is then given by:

$$\hat{\boldsymbol{v}}(\boldsymbol{\theta}) = \sum_{i=1}^{N} w_i(\boldsymbol{\theta}) \boldsymbol{v}_i, \tag{5.3}$$

with the weight $w_i(\boldsymbol{\theta})$ for each survey point expressed as:

$$w_i(\boldsymbol{\theta}) = \frac{\mathrm{K}_\theta(\frac{\boldsymbol{\theta}-\boldsymbol{\theta}_i}{h_\theta})}{\sum_{j=1}^{N} \mathrm{K}_\theta(\frac{\boldsymbol{\theta}-\boldsymbol{\theta}_j}{h_\theta})} \tag{5.4}$$

The value of h_θ determines the accuracy of the RSS estimation process in (5.4). The cross-validation approach discussed in Section 4.1 is used for obtaining the optimal kernel width h_θ. In this case, the cross-validation involves removing the random RSS vector of one point from the survey set and then estimating that RSS vector using the RSS vectors of the rest of the survey points and their respective locations. The cross-validation MSE for a RSS vector estimation is then:

$$\mathrm{MSE}_{cross} = \sum_{i=1}^{N} \left| \boldsymbol{v}_i - \sum_{k=1,\neq i}^{N} \boldsymbol{v}_k \tilde{w}_k^i(\boldsymbol{\theta}_i) \right|^2, \tag{5.5}$$

and a modified version of the weight function from (5.4) is obtained:

$$\tilde{w}_k^i(\boldsymbol{\theta}_i) = \frac{\mathrm{K}_\theta(\frac{\boldsymbol{\theta}_i-\boldsymbol{\theta}_k}{h_\theta})}{\sum_{j=1,\neq i}^{N} \mathrm{K}_\theta(\frac{\boldsymbol{\theta}_i-\boldsymbol{\theta}_j}{h_\theta})}. \tag{5.6}$$

In the following sections this method of estimating the RSS measurements is used for calibrating the RSS data obtained from two different laptops and from one of these laptops and various portable handsets.

5.2 Laptop to Laptop RSS Calibration

To pave the way for the RSS calibration for handsets, the first analysis of the RSS variation was conducted between two different laptop computers. The clustered set of the ECS fifth floor mentioned in Section 4.2 and a new clustered set collected with another laptop on the same floor are used for comparison of the RSS levels. Once the collection of new set was completed, the differences in the RSS mesurements were investigated. Fig. 5.1 shows the RSS variation in the two laptops for a sample of 52 locations.

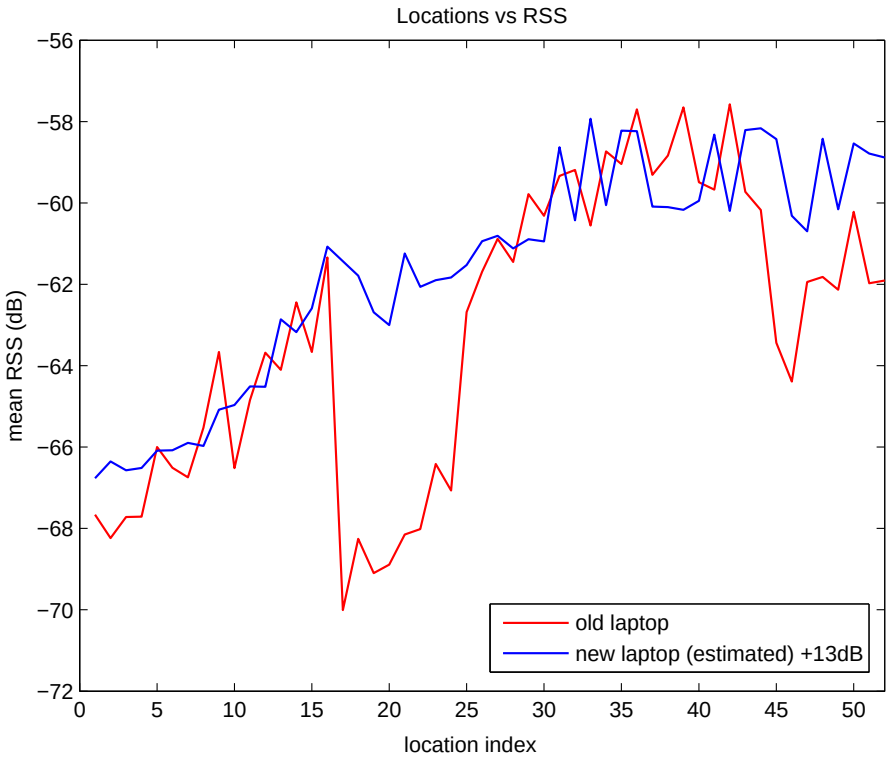

Figure 5.1: Location vs RSS for two laptops

In order to match the signal levels of the two laptop computers, it is proposed to multiply the new laptop's RSS by a constant k, such that $0 \leq k \leq 2$, and add a delta

to the result. Thus, an affine transformation was devised as a solution for matching the two sets of signals. An affine transformation between two vector spaces consists of a linear transformation and a translation, i.e.: $\boldsymbol{y} = \boldsymbol{A}\boldsymbol{x} + \boldsymbol{b}$. In our particular case, the transformation is expressed as:

$$\boldsymbol{V}'_{new} = k\,(\boldsymbol{V}_{new} - m_{new}) + m_{old} \tag{5.7}$$

where the subscripts *new* and *old* refer to the new and old laptops respectively. $\boldsymbol{V}_{new}$ are the RSS random vectors for all locations collected with the new laptop, $\boldsymbol{V}'_{new}$ are the converted RSS vectors for the same locations, and k, m_{new} and m_{old} are the parameters of the transformation. k represents a scaling constant, whereas m_{new} and m_{old} are translation constants. Based on the results shown in Fig. 5.1, m_{new} and m_{old} were selected to be: $m_{new} = \bar{\boldsymbol{V}}_{new} = -64.51$ dBm and $m_{old} = \bar{\boldsymbol{V}}_{old} = -64.34$ dBm. The best value of the scaling constant k was determined experimentally to be 0.79.

After obtaining the parameters for the affine transformation, the next step is to test this transformation in a localization process. For this purpose, the uniform and clustered survey sets mentioned in Section 4.2, which were collected with laptop # 1, are used as survey sets to locate the clustered data set collected with laptop # 2. For convenience laptop # 1 will be denoted *old* laptop and laptop # 2 *new* laptop. The kernel widths are calculated using cross-validation for the two survey sets to estimate the RSS vectors for the data set. Fig. 5.2 shows the value of h_θ for the clustered survey set found via the cross-validation technique. The RSS vectors are transformed using (5.7) and then used for localization. The localization process was performed with measurements from 9 WAPs. The results of the radio location are summarized in Table 5.1.

Fig. 5.3 shows that the estimated location is approximately within 325 cm of the true location for the clustered survey set 90% of the time and this distance is 400 cm for the uniform survey set when an affine transformation is used in both cases. On

Table 5.1: Radio Location Summary for Laptop to Laptop RSS Calibration

Survey Set	Test Set	h_v	h_{theta}	RMSE
Fifth Floor Clustered (Old)	Fifth Floor Clustered (New)	3.6	82 cm	164 cm
Fifth Floor Uniform (Old)	Fifth Floor Clustered (New)	3.4	62 cm	194 cm

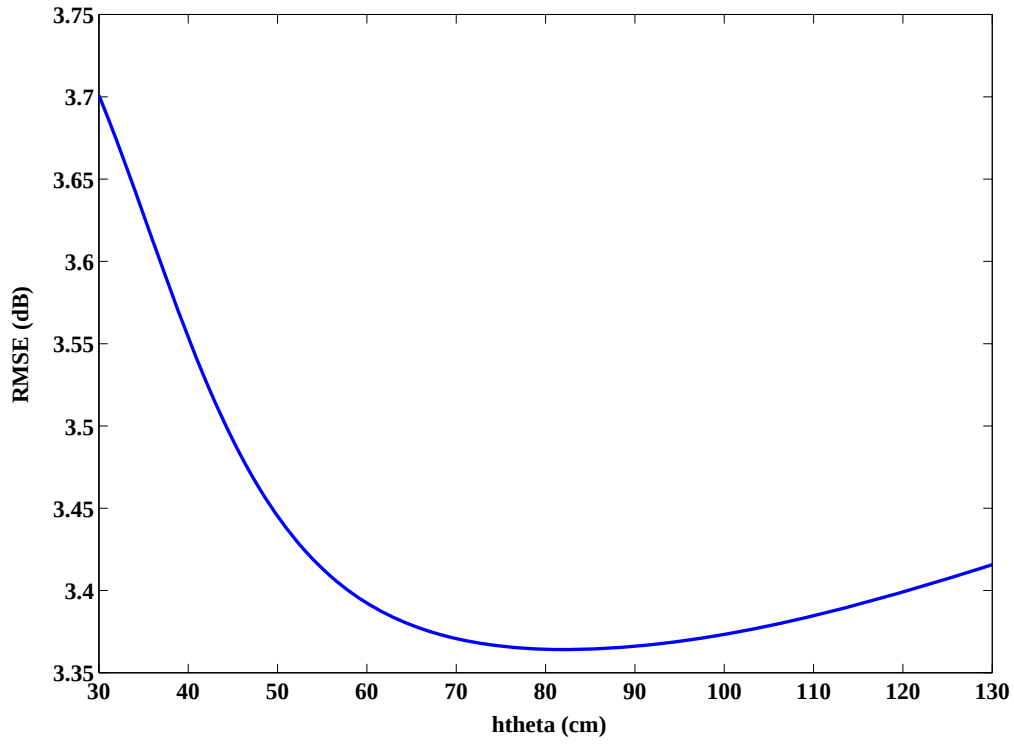

Figure 5.2: h_θ for the Clustered Survey Set (Old laptop)

the contrary, when no transformation is used for localization, in both the uniform and survey sets the estimated location is approximately within 750 cm of the true location 40% of the time. As it can be seen in Fig. 5.3, there is an improvement in location accuracy of almost one order of magnitude when a transformed survey set is used for localization as opposed to when a non-transformed survey set is used. Thus, it can be clearly seen that an affine transformation for the RSS measurements produces accurate localization results. The insight into the laptop to laptop calibration procedure gained in this section will be applied to the laptop to handsets calibration in the next section.

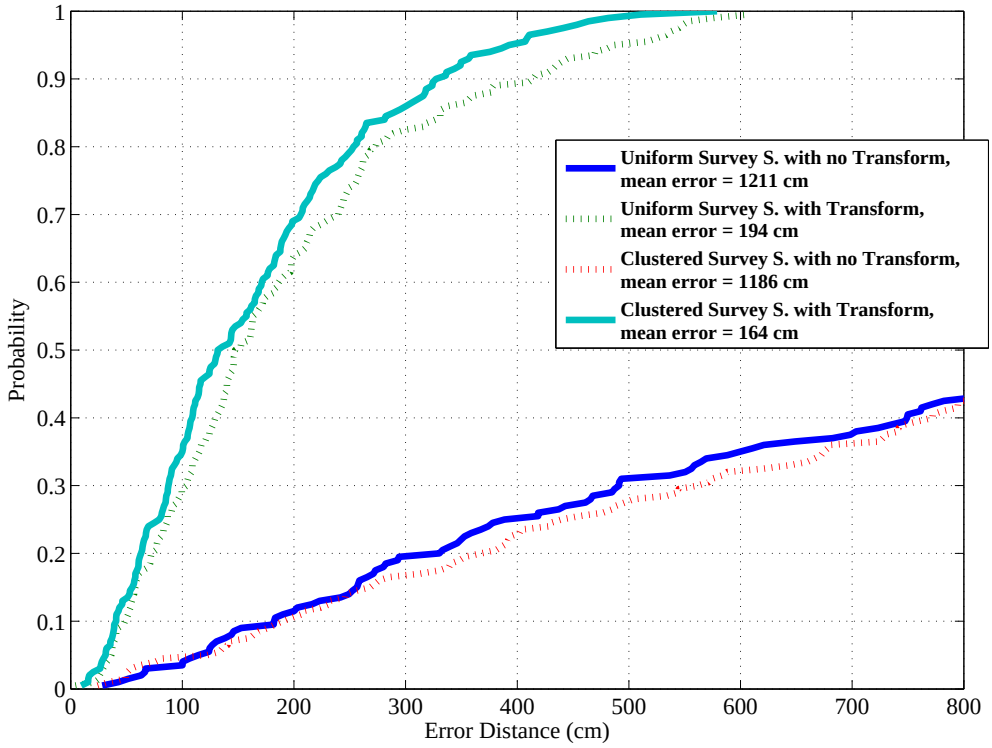

Figure 5.3: Location Accuracy for Laptop Calibration

5.3 Laptop to Handsets RSS Calibration

Locating test sets collected with a mobile handset using a survey set collected with a laptop becomes a more difficult problem than locating sets from different laptops. The increment in difficulty arises due to various factors, such as number and position of the Wi-Fi antennas as mentioned in the first paragraphs of this chapter. The orientation of these antennas with respect to an incoming signal is another cause of variation in the RSS levels [59].

In order to overcome these problems an experiment of laptop to handset calibration was planned. In this experiment 7 Nokia mobile phones lying on a flat position on top of a survey tray were used: two N95-1s, two N95-4s (N95 8GB North American Model), two N71-1s, and one N82-1. Data sets of 52 points covering half of the ECS fifth floor were collected in a uniform straight-line fashion for each of these phones. The RSS vectors of the phone data sets are calibrated to the RSS measurements of the uniform survey set mentioned in Section 4.2. Fig. 5.4 shows the RSS variation between the laptop and one of the N95-1 handsets.

It can be seen from Fig. 5.1 and 5.4 that the difference in the RSS levels between the old and new laptops and the old laptop and the N95-1 handset model are comparable. As a result, it is expected that the parameters of the transformation of the laptop to handset calibration are similar to those of the laptop to laptop calibration. The affine transformation of Section 5.2 can be restated as:

$$\boldsymbol{V}_h' = k\,(\boldsymbol{V}_h - m_h) + m_l \tag{5.8}$$

where the subscripts h and l stand for handset and laptop respectively. $\boldsymbol{V}_h$ are the RSS random vectors for all locations collected with a handset, $\boldsymbol{V}_h'$ are the converted RSS vectors for the same locations, and k, m_h and m_l are the parameters of the transformation. Note that the subscript *old* has been replaced by l for notation convenience, but they refer to the same data, i.e. the data coming from the old

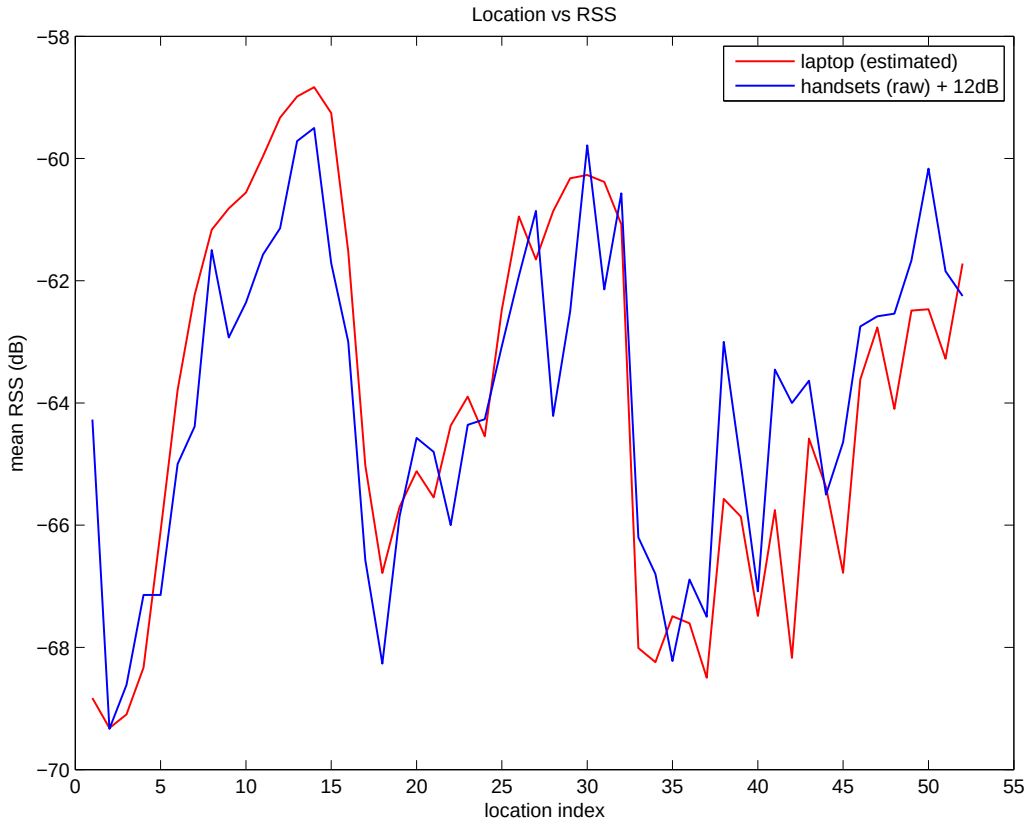

Figure 5.4: Location vs RSS for a laptop and a handset

laptop. Given the results shown in Fig. 5.1 and 5.4, m_h and m_l were chosen to be: $m_h = \bar{\boldsymbol{V}}_h = -64.5$ dBm and $m_l = \bar{\boldsymbol{V}}_l = -63.8$ dBm. To refine the calculation of k, an estimation procedure is proposed as the value of k that minimizes the MSE of the translation:

$$k = \arg\min_k \sum_N \left[k\left(\boldsymbol{V}_h - m_h\right) + m_l - \boldsymbol{V}_l\right]^2 \tag{5.9}$$

where N is the total number of RSS measurements in the data set. Fig. 5.5 depicts the RMSE variation for various values of k and it can be seen that the optimal value is 1.55.

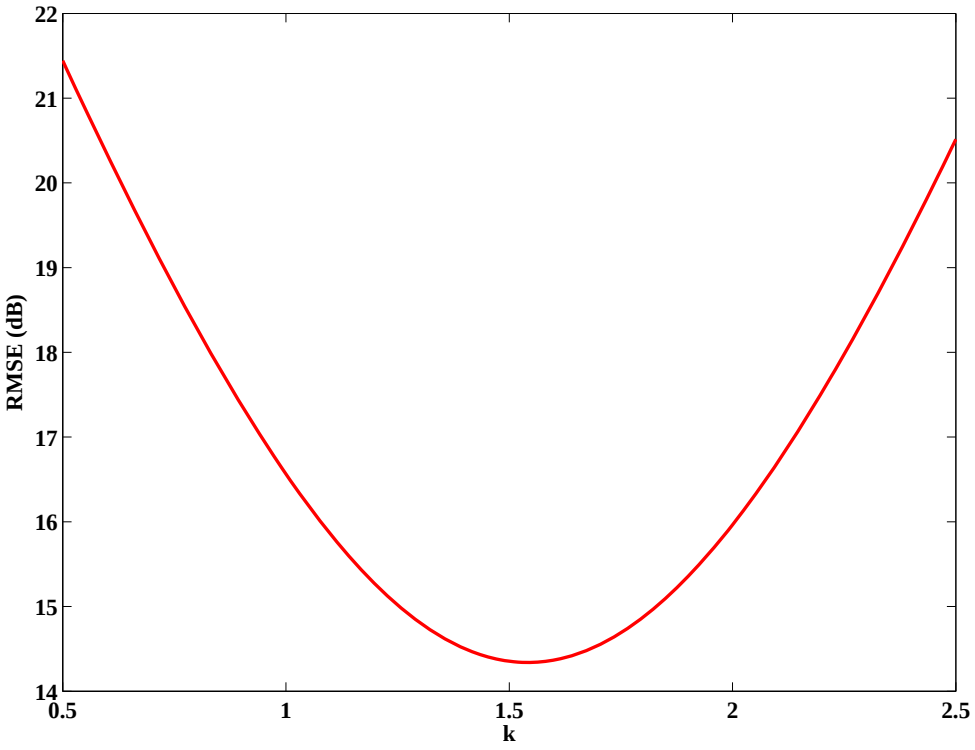

Figure 5.5: k vs RMSE of the affine function

In the localization phase, the uniform survey set of Section 4.2 is used to locate the 7 phone data sets. The kernel widths were determined via cross-validation, the RSS vectors were transformed using (5.8) and 10 WAPs were used. Fig. 5.6 shows that the distance error in handset localization is less than 2m for all 7 phones, which is consistent with the location accuracy for the new laptop. Despite the high degree of location estimation accuracy achieved, *a priori* knowledge of the data set's RSS measurements for all locations is required to determine the transformation parameters for every device that needs calibration. Therefore, an automated calibration method based on the Expectation-Maximization algorithm will be presented in the following section. The proposed technique is an online solution that requires only a few locations to determine the affine function parameters.

5.4 Automated Calibration

5.4.1 Expectation Maximization Algorithm

The Expectation Maximization (EM) algorithm is an iterative optimization method to compute MLEs of the parameters of an underlying distribution from a given data set when the observed measurement data vector $\boldsymbol{X}$ is considered as incomplete and is seen as an observable function of the complete data [60, 61]. The computation of MLEs requires estimating unknown parameters $\boldsymbol{\Psi}$ given measurement data $\boldsymbol{X}$. In particular, the posterior probability of the parameters $\boldsymbol{\Psi}$ needs to be maximized given the data $\boldsymbol{X}$ and marginalized over hidden variables $\boldsymbol{Y}$ [62], such that:

$$\Psi^* = \arg\max_{\Psi} \sum_{\boldsymbol{Y} \in \mathrm{Y}^n} P\left(\boldsymbol{\Psi}, \boldsymbol{Y} | \boldsymbol{X}\right). \tag{5.10}$$

On each iteration of the EM algorithm, there are two steps: the expectation step or E-step and the maximization step or M-step. This is the reason why the algorithm is called the EM algorithm. One of the most insighful explanations of EM is in terms

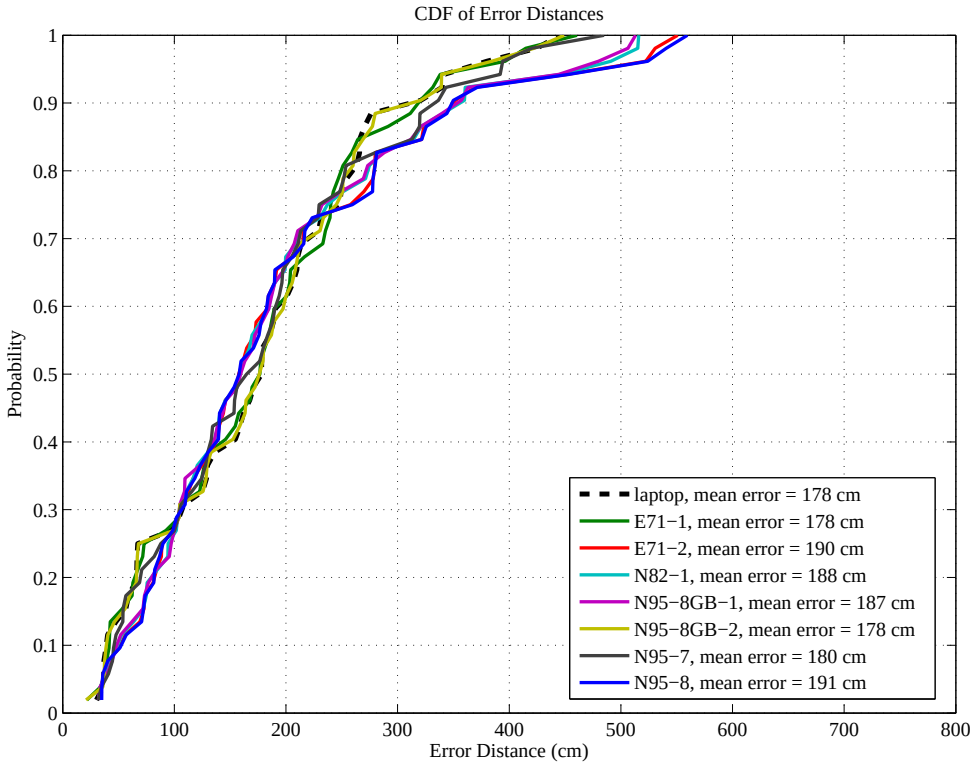

Figure 5.6: Location Accuracy for Handset Calibration

of lower bound maximization. The E-step can be seen as a process of finding a local lower bound to the posterior distribution, whereas the M-step optimizes the bound, thereby improving the estimate of the unknowns [63], [64]. The maximization in (5.10) can be equivalently written as a maximization of the logarithm of the joint distribution function:

$$\Psi^* = \arg\max_{\Psi} \log P\left(\boldsymbol{X}, \boldsymbol{\Psi}\right) = \arg\max_{\Psi} \log \sum_{\boldsymbol{Y} \in \mathrm{Y}^n} P\left(\boldsymbol{X}, \boldsymbol{Y}, \boldsymbol{\Psi}\right). \tag{5.11}$$

The key concept behind EM is to begin with an initial guess $\boldsymbol{\Psi}^t$ for the parameters $\boldsymbol{\Psi}$, compute an easily calculated lower bound $B\left(\boldsymbol{\Psi}, \boldsymbol{\Psi}^t\right)$ to the function $\log P\left(\boldsymbol{\Psi}|\boldsymbol{X}\right)$, and maximize that bound instead. The bound improves at each iteration, so this process will converge to a local maximizer $\boldsymbol{\Psi}^*$ of the objective function. The EM can be then summarized as [62]:

- E-step: calculate $f^t(\boldsymbol{Y}) \equiv P\left(\boldsymbol{Y}|\boldsymbol{X}, \boldsymbol{\Psi}^t\right)$
- M-step: $\boldsymbol{\Psi}^{t+1} = \arg\max_{\Psi} \left[Q^t(\boldsymbol{\Psi}) + \log P(\boldsymbol{\Psi})\right]$

In the M-step, $Q^t(\boldsymbol{\Psi})$ is the expected complete log-likelihood, i.e. $Q^t(\boldsymbol{\Psi}) = \langle \log P\left(\boldsymbol{X}, \boldsymbol{Y}|\boldsymbol{\Psi}\right)\rangle$ as defined in [61], [65]

.

5.4.2 Expectation Maximization for Automated Calibration

Based on the general notion of the EM presented in 5.4.1, an algorithm for automated laptop to handset RSS calibration will be described. It is important to note that since m_l is a parameter obtained from the survey set of RSS measurements collected with the old laptop, which are known *a priori*, the automated calibration needs to be performed only for the remaining two parameters, k and m_h. The automated calibration algorithm requires known locations of a handset and the respective RSS

data at these locations as inputs. The algorithm simultaneously locates the phone and calibrates the localization system. The variable sets for our EM algorithm are:

- Observations $\boldsymbol{X}$: RSS measurement vector at the current location.
- Parameters: $\boldsymbol{\Psi} = (k, m_h)$.
- Hidden variables $\boldsymbol{Y}$: Current handset location for $\boldsymbol{X}$.

The steps of the algorithm are the following:

E-step:

1. Select one location from previously collected phone data set, i.e. a known location, and its respective RSS measurement vector $\boldsymbol{V}_h$. This known location needs to be near the current handset location.
2. Given that $\boldsymbol{\Psi^t} = (k^t, m_h^t)$, where t is the current iteration, estimate the RSS measurement vector for the location selected in step 1 with (5.3) and convert it using (5.8). The reason to estimate and convert this RSS value is because the available RSS from an old data set was collected with a laptop. The initial values of the parameters are: $\boldsymbol{\Psi^1} = (k^1, m_h^1) = (1.2, -58.2 \text{ dBm})$.
3. Estimate the location of this handset point with (4.6).
4. Match this point to possible survey point locations by comparing RSS values in the base stations. Choose the most likely survey location match by selecting the lowest Root Mean Squared Error (RMSE) between the estimated location from step 3 and the possible survey point true locations, so that the function $f^t(\boldsymbol{Y}) \equiv P(\boldsymbol{Y}|\boldsymbol{X}, \boldsymbol{\Psi}^t)$ is obtained.

M-step:

5. Use the RSS of the most likely survey point and the RSS handset measurement from step 1 to obtain new values for k and m_h by a least squares minimization of the function:

$$\Psi^{t+1} = \arg \min_{(k^t, m_h^t)} \sum_{N} \left[k^t \left(\boldsymbol{V}_h - m_h^t \right) + m_l - \boldsymbol{V}_l \right]^2 \tag{5.12}$$

   where $\boldsymbol{V}_l$ is the RSS vector of measurements of the most likely survey set location and N is the number of RSS measurements in $\boldsymbol{V}_l$ at that location.

6. With k and m_h from step 5 go back to step 1 and accumulate the selected RSS vectors of measurements from previous iterations. N in (5.12) is then the total number of RSS measurements in all vectors $\boldsymbol{V}_l$ at the selected locations.

The automated calibration algorithm converged to $k = 1.55$ and $m_h = -64.4$ dBm as the process was iterated for 11 locations in a mobile phone data set. It can be then concluded that the number of locations needed to determine the optimal affine function parameters is in the neighborhood of 11 if adequate values are chosen for the initial values of the parameters.

Chapter 6
Conclusion

In this thesis, novel solutions for technical challenges in an indoor location fingerprinting system were presented. Using a robust statistical method, the negative influence of outliers found in distance measurements in listener sensor localization was reduced. Second, a spatial domain filter has been used to remove the noise component caused by multipath propagation. The location accuracy with this filtering technique was reduced to less than 2m. Finally, an automated calibration method between the RSS from a laptop and several handsets was introduced using an affine transformation. This technique allowed to reach accuracy levels of less than 2m for handset localization. This chapter summarizes the problems investigated and the particular achievements of this work.

6.1 Thesis Summary

In Chapter 2 a description of the data collection technique with the use of a ultrasonic sensor network is given and the Cricket localization algorithm is explained. Robust Statistics is then introduced as a potential tool to reduce the error caused by NLoS distance measurements obtained when the sensors are placed on walls in hallways. The conventional Huber window is described to serve as a plataform for modifications according to the specific needs of our problem. The ρ and ψ functions of a robust window are identified. A modified Huber window is then developed based on the pattern of the distance data. The achievement in this chapter is the reduction of the Cricket mean distance error to 7.4 cm.

In Chapter 3 a description of the basic funcionality of the Wiener filter and its

application to noise reduction is presented. In addition, the strengths and weaknesses of the most common filtering technique in the noise reduction literature, time domain averaging, are clearly determined. To overcome the deficiencies of the time domain or median filter, in particular the inability to remove multipath propagation noise, a spatial domain averaging technique is developed. The noise removal algorithm parameters, d and σ^2 are defined.

Chapter 4 describes how the survey data is used to create an accurate WLAN location fingerprinting system. A Parzen Window Estimator is developed as an approximation of the MMSE estimator to be used for mobile terminal localization. The method to determine the estimation algorithm parameter or kernel width, h_v, is explained. Furthermore, a cross-validation approach is presented as a less expensive alternative to the determination of h_v. The cross-validation technique is then extended for calculation of the noise removal parameters d and σ^2 as well.

The testbed for radio location is located on the sixth and fifth floors of the ECS. Two point sets were used as survey sets to determine the best distribution of points in a survey set. In one set the locations were uniformly distributed over the network area in a straight-line fashion. In the second set the locations were collected in tight clusters of four points each. The noise removal technique was then applied to clustered survey sets from the fifth and sixth floors. It was shown that the improvement in localization accuracy was 16% in the fifth floor and 11% in the sixth floor. It was also pointed out that the clustered survey set provides accuracy improvements to the uniform set even when no spatial averaging is performed.

In Chapter 5 the problem of calibrating the RSS measurements collected with several mobile devices is investigated. The importance of an automated calibration method is highlighted. A procedure to estimate the RSS measurements of a data set using the locations of the mobile terminal is developed as the basis for the calibration technique, where the kernel width h_θ needs to be calculated. First, a laptop to

laptop calibration is studied and an affine transformation is proposed as a solution for matching the signal levels between the two devices. The parameters of the transformation, k, m_{new} and m_{old} were determined through an analysis of the RSS data from the two laptops. The localization accuracy levels were below 2m when both the uniform and clustered sets from the fifth floor were used as survey sets to locate a calibrated clustered set collected with the new laptop. This indicated that the use of an affine transformation was an adequate method for signal calibration.

The second study involved calibrating the RSS levels between a laptop and 7 mobile phones. The translation parameters, m_h and m_l of the affine function were defined analyzing the RSS levels from the old laptop and a N95-1 handset model. The scaling constant, k, was calculated through an estimation procedure that minimizes the MSE of the translation. The uniform survey set from the fifth floor was then used to locate the data sets of the 7 cellular phones. The handset localization process yielded an accuracy of less than 2m. Finally, an automated calibration process based on the EM algorithm was presented. This technique is an online solution that requires a few locations to determine two of the affine transformation parameters, k and m_h, since m_l is known a priori. It was shown that only 11 locations were needed to make the automated calibration algorithm converge to the optimal transformation parameters.

6.2 Major Contributions

The major contributions of this thesis are summarized below:

1. **Robust Window:** The development of a robust window function to decrease the infuence of outliers in the localization of the listener sensor in the data collection phase. The error in the listener localization with this robust method was reduced to 7.4 cm. This result allows the use of a sensor network as an

effective tool for data collection purposes.

2. **Noise Reduction:**

   - The introduction of a spatial domain noise removal technique to reduce time-invariant measurement noise caused by the multipath propagation effect.
   - The demostration that survey data collected in tight clusters of locations as opposed to uniformly distributed over the network area facilitates efficient noise removal and hence improves the localization accuracy.
   - The use of an inexpensive cross-validation method to determine the parameters of the noise removal and location estimation algorithms from survey data.

3. **Automated Calibration:**

   - The development of an algorithm to estimate the RSS measurements of a data set using the locations of the mobile terminal.
   - The definition of an affine transformation as a RSS calibration method between two laptops and a laptop and several mobile phones. It was demonstrated that the use of an affine function allowed to have a high degree of accuracy in the localization phase.
   - The development of an online automated calibration process that needs a few number of locations to define the optimal transformation parameters.

6.3 Future Research Directions

This thesis has addressed various technical challenges of WLAN localization; however, several problems remain to be investigated. These are presented below:

- A study of other robust methods for listener sensor localization to determine the most efficient in terms of outlier rejection and algorithm implementation.

- The use of dinamically built radio maps based on real-time enviromental sensing to mitigate the arduous efforts of the data collection phase. Recent work [28] aims to address this technique. Nonetheless, intensive further research lies ahead in this area.

- The number of points in a each tight cluster for optimal noise removal and the best geometry of the cluster locations needed to obtain the highest localization accuracy require further experimental investigation. A comparison of point sets with different cluster sizes and different cluster geometries would be the most adequate scenario to define the optimal data collection point distribution for localization purposes with spatial filtering.

- The types on contextual services that could potentially be offer to mobile customer once this level of localization accuracy (less than 2m) for laptop and handsets has been achieved. Highly accurate localization opens up the door for a plethora of location-aware services that need to be either refined or materialized.

Bibliography

[1] M. Hazas, J. Scott, and J. Krumm, "Location-aware computing comes of age," *IEEE Computer*, vol. 37, no. 2, pp. 95–97, 2004.

[2] A. Huang and L. Rudolph, "An infrastructure for location aware computing," In Proceedings of the 2004 Student Oxygen Workshop, MIT Computer Science and Artificial Intelligence Laboratory, Cambridge MA, USA, Workshop, 2004.

[3] EKahau, available online at: http://www.ekahau.com. Accessed: September 2009.

[4] "Wi-fi based real-time location tracking: Solutions and technology. CISCO sytems." available online at: http://www.cisco.com. Accessed: September 2009.

[5] T. Roos, M. Myllymki, H. Tirri, P. Misikangas, and J. Sievnen, "A probabilistic approach to WLAN user location estimation," *International Journal of Wireless Information Networks*, vol. 9, no. 3, pp. 155–164, 2002.

[6] M. Rodriguez, J. Favela, E. Martinez, and M. Munoz, "Location-aware access to hospital information and services," *IEEE Transactions on Information Technology in Biomedicine*, vol. 8, no. 4, pp. 448–455, 2004.

[7] H. Harroud, M. Ahmed, and A. Karmouch, "Policy-driven personalized multimedia services for mobile users," *IEEE Trans. Mobile Comput.*, vol. 2, no. 1, pp. 16–24, 2003.

[8] C. Patterson, R. Muntz, and C. Pancake, "Challenges in location-aware computing," *IEEE Pervasive Comput.*, vol. 2, no. 2, pp. 80–89, 2003.

[9] I. Getting, "The global positioning system," *IEEE Spectrum*, vol. 30, no. 12, pp. 36–47, 1993.

[10] T. Kerr, "A critical perspective on some aspects of gps development and use," *Proc. AIAA/IEEE Digital Avionics Systems Conference*, vol. 2, pp. 9.4–9–9.4–20, October 1997.

[11] F. van Diggelen, "Indoor GPS theory and implementation," in *Proc. IEEE Position Position, Location and Navigation Symposium*, April 2002, pp. 240–247.

[12] G. Dedes and A. Dempster, "Indoor GPS positioning - challenges and opportunities," in *Proc. IEEE Vehicular Technology Conf.*, September 2005, pp. 412–415.

[13] A. Sayed, A. Tarighat, and N. Khajehnouri, "Network-based wireless location: challenges faced in developing techniques for accurate wireless location information," *IEEE Signal Processing Mag.*, vol. 22, no. 4, pp. 24–40, 2005.

[14] G. Sun, J. Chen, W. Guo, and K. Liu, "Signal processing techniques in network-aided positioning: a survey of state-of-the-art positioning designs," *IEEE Signal Processing Mag.*, vol. 22, no. 4, pp. 12–23, 2005.

[15] R. Want, A. Hopper, V. Falcao, and J. Gibbons, "The active badge location system," *ACM Trans. Information Systems*, vol. 10, no. 1, pp. 91–102, January 1992.

[16] R. Want, B. Schilit, N. Adams, R. Gold, K. Petersen, D. Goldberg, J. Ellis, and M. Weiser, "An overview of the parctab ubiquitous computing experiment," *IEEE Personal Comm. Magazine*, vol. 2, no. 2, pp. 28–33, December 1995.

[17] D. Kirsh and T. Starner, "The locust swarm: An environmentally-powered, networkless location and messaging system," in *Proc. First Intl Symp. Wearable Computers*, Oct. 1997.

[18] X. Li and K. Pahlavan, "Super-resolution TOA estimation with diversity for indoor geolocation," *IEEE Transactions on Wireless Communications*, vol. 3, no. 1, pp. 224–234, 2004.

[19] C. Randell and H. Muller, "Low cost indoor positioning system," in *Proc. Ubicomp 2001: Ubiquitous Computing*, September 2001.

[20] D. Niculescu and B. Nath, "VOR base stations for indoor 802.11 positioning," in *Mobi-Com '04: Proceedings of the 10th Annual International Conference on Mobile computing and networking*, 2004, pp. 58–69.

[21] P. Bahl and V. Padmanabhan, "RADAR: An in-building RF-based user location and tracking system," in *Proc. IEEE Conf. Computer Comm. (INFOCOM)*, vol. 2, 2000, pp. 775–784.

[22] M. McGuire and K. Plataniotis, "Estimating position of mobile terminals from path loss measurements with survey data," *Wireless Communications and Mobile Computing*, vol. 3, no. 1, pp. 51–62, February 2003.

[23] M. Youssef and A. Agrawala, "Continuous space estimation for WLAN location determination systems," in *IEEE Thirteenth International Conference on Computer Communications and Networks*, 2004.

[24] C.-D. Wang, M. Gao, and X.-F. Wang, "An 802.11 based location-aware computing: Intelligent Guide System," in *International Conference on Communications and Networking in China, 2006. ChinaCom '06*, October 2006, pp. 1–5.

[25] M. Youssef and A. Agrawala, "The Horus WLAN location determination system," in *International Conference on Mobile Systems, Applications, and Services (MobiSys)*, June 2005.

[26] X. Chai and Q. Yang, "Reducing the callibration effort for probabilistic indoor location estimation," *IEEE Transactions on Mobile Computing*, vol. 6, no. 6, pp. 649–662, June 2007.

[27] A. Kushki, K. Plataniotis, and A. Venetsanopoulos, "Kernel-based positioning in wireless local area networks," *IEEE Trans. Mobile Comput.*, vol. 6, no. 6, pp. 689–705, June 2007.

[28] J. Yin, Q. Yang, and L. Ni, "Learning adaptive temporal radio maps for signal-strength-based location estimation," *IEEE Trans. Mobile Comput.*, vol. 7, pp. 869–883, July 2008.

[29] A. Nafarieh and J. How, "A testbed for localizing Wireless LAN devices using received signal strength," in *6th Annual Communication Networks and Services Research Conference*, May 2008, pp. 481–487.

[30] A. Kushki, "A cognitive radio tracking system for indoor environments," Ph.D. dissertation, University of Toronto, 2008.

[31] J. Parsons, *The Mobile Radio Propagation Channel (2nd ed.)*. West Sussex, England: John Wiley & Sons, Inc., 2000.

[32] K. Kaemarungsi, "Design of indoor positioning systems based on location fingerprinting technique," Ph.D. dissertation, University of Pittsburgh, 2005.

[33] M. Youssef, A. Agrawala, and A. Shankar, "WLAN location determination via clustering and probability distributions," in *Proc. First IEEE Intl Conf. Pervasive Computing and Comm.*, 2003, pp. 143–150.

[34] M. McGuire, K. Plataniotis, and A. Venetsanopoulos, "Location of mobile terminals using time measurements and survey points," *IEEE Trans. Veh. Technol.*, vol. 52, no. 4, pp. 999–1011, July 2003.

[35] E. Hyun, "An indoor-location sensing system using WLAN and ultrasonic/radio technologies," Master's thesis, University of Victoria, 2008.

[36] N. Priyantha, A. Miu, H. Balakrishnan, and S. Teller, "The cricket compass for context-aware mobile applications," in *Proc. Seventh Intl Conf. Mobile Computing and Networking (MobiCom)*, July 2001.

[37] D. Arora, D. Felix, and M. McGuire, "Reducing the error in mobile location estimation using robust window functions," in *IEEE Pacific Rim Conference on Communications, Computers and Signal Processing (PacRim)*, August 2009.

[38] M. Youssef and A. Agrawala, "Handling samples correlation in the Horus system," in *INFOCOM*, 2004, pp. 1023–1031.

[39] A. Krishnakumar and P. Krishnan, "On the accuracy of signal strength-based estimation techniques," in *INFOCOM*, 2005, pp. 642–650.

[40] H. Lim, L. chuan Kung, J. Hou, and H. Luo, "Zero-configuration, robust indoor localization: Theory and experimentation," in *INFOCOM*, 2006.

[41] R. Battiti, T. Nhat, and A. Villani, "Location-aware computing: a neural network model for determining location in wireless LANs," Department of Information and Communication Technology, University of Trento, Italy, Tech. Rep. DIT-02-0083, 2002.

[42] S.-H. Fang and T.-N. Lin, "Robust wireless LAN location fingerprinting by SVD-based noise reduction," in *International Symposium on Communications, Control and Signal Processing (ISCCSP)*, March 2008.

[43] R. Steele, *Mobile Radio Communications*. IEEE Press, 1992.

[44] J. Krumm, E. Horvitz, and A. Shankar, "LOCADIO: Inferring motion and location from wi-fi signal strengths," in *Proc. ACM International Conference on Mobile and Ubiquitous Systems: Networking and Services (MOBIQUITOUS'04)*, Boston, MA, August 2004.

[45] N. Priyantha, "The Cricket indoor location system," Ph.D. dissertation, Masachusetts Institute of Technology, June 2005.

[46] MIT Computer Science and Artificial Intelligence Lab, *Cricket V2 User Manual*, January 2005.

[47] R. Maronna, R. D. Martin, and V. Yohai, *Robust Statistics Theory and Methods*, ser. Wiley Series in Probability and Statistics. John Wiley & Sons, Inc., 2006.

[48] W. Frank, R. Hampel, P. Rousseeuw, and E. Ronchetti, *Robust Statistics: The Approach Based on Influence Functions*, 1st ed. John Wiley & Sons, Inc., 1986.

[49] J. P. Huber, *Robust Statistics*, 1st ed. John Wiley & Sons, Inc., 1981.

[50] S. Haykin, *Adaptive Filter Theory*, 3rd ed. Prentice Hall, 1996.

[51] S. Vaseghi, *Advanced Digital Signal Processing and Noise Reduction*, 2nd ed. John Wiley & Sons, 2000.

[52] M. Gudmundson, "Correlation model for shadow fading in mobile radio systems," *Electron. Lett.*, vol. 27, pp. 2145–2146, 1991.

[53] E. Hyun, M. McGuire, and M. Sima, "Radloco: A rapid and low cost indoor location-sensing system," in *Proc. International Conference on Communications and Networking in China (Chinacom)*, August 2008, pp. 630–634.

[54] J. M. Mendel, *Lessons in Estimation Theory for Signal Processing, Communications, and Control*, 2nd ed. Englewood Cliffs, NJ: Prentice-Hall, 1995.

[55] D. Scott, *Multivariate Density Estimation: Theory, Practice, and Visualization*, ser. Wiley Series in Probability and Statistics. Wiley-Interscience, September 1992.

[56] B. W. Silverman, *Density estimation for statistics and data analysis*, ser. Monographs on Statistics and Applied Probability. London: Chapman and Hall, 1986.

[57] F. Ramos, B. Upcroft, S. Kumar, and H. Durrant-Whyte, "A Bayesian approach for place recognition," in *ICJAI Workshop Reasoning with Uncertainty in Robotics*, Edinburgh, Scotland, July 2005.

[58] R. O. Duda, P. E. Hart, and D. G. Stork, *Pattern Classification*, 2nd ed. John Wiley & Sons, Inc., 2001.

[59] C. Pearson, M. McGuire, and Y. Coady, "The application of Wi-Fi radiolocation research to mobile devices," in *IEEE Pacific Rim Conference on Communications, Computers and Signal Processing (PacRim)*, August 2009.

[60] J. Bilmes, "A gentle tutorial of the EM algorithm and its application to parameter estimation for gaussian mixture and hidden markov models," International Computer Science Institute and Computer Science Division, Department of Electrical Engineering and Computer Science, University of California at Berkeley, Berkeley, CA, USA, TR-97-021, 1998.

[61] G. McLachlan and T. Krishnan, *The EM algorithm and extensions*, ser. Wiley Series in Probability and Statistics. John Wiley & Sons, Inc., 1997.

[62] F. Dellaert, "The Expectation Maximization algorithm," Georgia Institute of Technology College of Computing, Tech. Report GIT-GVU-02-20, 2002.

[63] T. Minka, "Expectation-Maximization as lower bound maximization."

[64] R. Neal and G. Hinton, *A view of the EM algorithm that justifies incremental, sparse, and other variants*. Kluwer Academic Press, 1998, in Jordan, M. editor, Learning in Graphical Models.

[65] A. Dempster, N. Laird, and D. Rubin, "Maximum likelihood from incomplete data via the EM algorithm," *Journal of the Royal Statistical Society*, vol. 39, no. 1, pp. 1–38, 1977.

Partial Copyright License

Title of Thesis:

Received Signal Strength Calibration for Wireless Local Area Network Localization

Author: _____

Diego Felix

Signed: July 22, 2010